Korean J. Chem. Eng., 39(10), 2571-2593 (2022)
DOI: 10.1007/s11814-022-1201-5

pISSN: 0256-1115
eISSN: 1975-7220

REVIEW PAPER

Recent advances on the coconut shell derived carbonaceous material for the removal of recalcitrant pollutants: A review

Amy Aynee Chan*, Archina Buthiyappan, Abdul Aziz Abdul Raman*,†, and Shaliza Ibrahim****

*Department of Chemical Engineering, Faculty of Engineering, Universiti Malaya, 50603 Kuala Lumpur, Malaysia
**Institute of Ocean and Earth Sciences (IOES), Universiti Malaya, 50603, Kuala Lumpur Malaysia
(*Received 27 November 2021 • Revised 28 April 2022 • Accepted 6 June 2022*)

Abstract−Adsorption is a prominent and cost-effective water treatment method that has been used to remove a variety of contaminants due to its efficacy, ease of use, and environmental friendliness. Biosorbents developed from agricultural wastes have been extensively studied. This review gives insight into the potential of carbonaceous coconut shells as a source of biomass material to prepare adsorbents for wastewater treatment. The feasibility of coconut shells as a precursor material is beneficial for extensive industrial-scale applications due to their natural properties and long-term availability. This review article also illustrates the excellent adsorption performance of adsorbents derived from coconut shells that can be an alternative precursor to commercial carbons with a high market price. This review points out the applications of coconut shell-based adsorbents in removing a wide range of contaminants and actual industrial wastewater. Additionally, literature shows that modified coconut shell-based adsorbents show better adsorption performance in removing hazardous pollutants due to enhancement in adsorbents' structural characteristics. The discussion on the environmental and economic perspectives on utilizing coconut shell-based adsorbents is also of the highlights of this review. It is prospective for industries to explore converting agricultural wastes into low-cost green adsorbents for wastewater treatment.

Keywords: Biosorbent, Waste Biomass, Heavy Metal, Wastewater, Adsorption

INTRODUCTION

The agricultural sector is crucial to economic transformation as it is a powerful tool for ending poverty, providing food security and raw materials for various applications [1]. The agriculture sector's contribution to Gross Domestic Product (GDP) at the ASEAN level ranges from 0.03 to 22.8% and Malaysia is ranked eighth out of all the ASEAN countries. In 2020, the agriculture sector contributed 7.4% to Malaysia's GDP. The total agricultural exports increased to RM118.6 billion in 2020 from RM115.5 billion in the previous year [2]. Therefore, the agriculture sector has been indicated as a potential source of high capital investment and employment opportunities. However, agricultural activity is one of the main sectors that produce significant waste from their multiple processes, including preparation, storage, processing, depending on the agricultural products. Agricultural solid wastes can be classified into food processing solid waste, crop production solid waste, chemical waste, and industrial agricultural solid waste. About 1.2 million tons of agricultural wastes are disposed of in Malaysia's landfills annually. And Malaysia is expected to generate 0.21 kg/cap/day of agriculture waste in 2025 [3]. Malaysia is the second largest exporter or producer of palm oil in the world, which recorded 99.07 million tons in 2019 [4]. The massive plantation of oil palm accounts for about 5.4 million hectares contributing to about 90% of overall lignocellulosic biomass wastes in Malaysia [5]. Besides oil palm, Malaysia is also one of the important exporters of coconut products. The production of coconuts is mainly for heat and electricity supply, organic fertilizer, animal feeds, health drinks, etc. However, most of the biomass residues are not treated properly but abandoned at the site to decompose naturally or subjected to open burning, which causes severe water and air pollution [6]. To overcome the challenges in handling the waste disposal problem, the approach of converting these biomass wastes into significant materials for industrial application has been dedicated. With this, sustainable energy can be maintained and cleaner environment can be sustained.

Recently, agricultural wastes have been widely explored as a precursor in developing green adsorbents for wastewater treatment due to environmental considerations. There are several methods mainly used for wastewater treatment, including coagulation, flocculation, Fenton-like process, nano-filtration, osmosis, and adsorption [7]. Among all the techniques, adsorption process shows excellent potential in recalcitrant wastewater treatment because of its practicality, simplicity, cost-effectiveness, and sludge-free method [8-12]. Many conventional sorbents, including zeolite, fly ash, chitin, and activated carbon (AC), have been utilized for wastewater treatment. Among them, AC is preferred due to having various functional groups on surface, large surface area, and high porosity. Any low cost and eco-friendly materials that are rich in carbon content and have low ash content can be developed as carbon-based adsorbent for wastewater remediation. Different types of agricultural wastes have been utilized for the scavenging of dyes from

†To whom correspondence should be addressed.
E-mail: azizraman@um.edu.my

wastewater under different operating conditions. The potential of pomegranate fruit peels has been investigated as a low/zero cost precursor to develop AC for sequestering Methylene Blue (MB) dye from aqueous solution, as reported by Ahmad et al. [13]. Moreover, effective removal of Crystal Violet (CV) dye by biochar developed from mango leaves has been also reported by Vyavahare et al. [14]. This study howed that 99.85% of maximum CV dye adsorption achieved by biochar derived from mango leaves, which justified the potential of mango leaves as a feedstock mterial to treat contaminated wastewater. Oribayo et al. [15] and Hoang et al. [16] utilized coconut shell (CS) as a source of material to develop AC for the removal of MB and Rhodamine B dyes with cationic properties. The maximum adsorption capacity of MB and Rhodamine B dyes over coconut shell activated carbon (CSAC) was 320.5 mg/g and 94.08 mg/g, respectively. Other than dyes, the ability CS-derived adsorbent to remove sodiumdodecyl benzene sulfonate [17], lead (II) ions [18] and POME [19] from aqueous solution has been studied by in the past years. These studies revealed that CS demonstrated good adsorption performance on the removal of these chemical substances due to its excellent natural structure. All of these studies showed that biomass wastes can be alternative precursors to existing commercial carbons for recalcitrant wastewater treatment.

Chemical structures such as pores, hydroxyl group, methyl group, and carbonyl group add value to the utilization of agricultural CS [20]. CS also has a high content of carbon, is abundantly available, with low ash level, high volatile content, and high hardness, which validates that it is a suitable precursor to develop biomass based adsorbents [21]. Therefore, this article reviewed the recent advances of carbonaceous CS as a precursor in synthesizing adsorbents to remove pollutants from wastewater. This review also focuses on providing the different synthesis methods of CS-based adsorbents. In addition, it gives insight into the overview of significant effects of modification on the adsorbent structure, such as changes in total pore volume, specific surface area, removal percentage, and adsorption capacity in removing pollutants. Lastly, this review summarizes the environmental and economic perspectives of utilizing CS-based adsorbents.

BIOMASS-BASED ADSORBENT

Agricultural and plant-based wastes have shown good bio-sorption potential for heavy metal ions, dyes, persistent organic pollutants, pesticides, pharmaceutical waste and other recalcitrant pollutants. Some important features of biomass waste make it an ideal option for developing adsorbents, including the presence of cellulose, hemicellulose, and lignin [22]. Cellulose and hemicellulose contain hydroxyl, ether, and carbonyl functional groups, which are highly biodegradable, reusable, high melting point polymers and insoluble in most solvents due to the high crystallinity of structure and hydrogen bonding that links the structure. Additionally, carbonyl, methoxyl, and hydroxyl groups are important in determining the hydrophobicity or hydrophilicity of adsorbents and their adsorptive mechanism [23]. Therefore, all these functional groups play a significant role in achieving high dye adsorption. Various types of biomass wastes, including biomass leaves, fruit peels, crop stalks, and seed/nutshells, are widely used to synthesize biosorbents.

Guerrero-Coronilla et al. [24] studied the preparation of adsorbents from water hyacinth leaves to treat anionic amaranth dye along with the isotherm, kinetic and thermodynamic studies. They reported that 70 mg/g of maximum biosorption capacity was achieved using an adsorbent developed from water hyacinth leaves [24]. The Langmuir isotherm and pseudo-second-order kinetic model best represented the equilibrium data, which suggests a monolayer chemisorption process on the homogeneous layer. The positive values obtained for the changes in activation enthalpy and Gibbs free energy revealed that the process was endothermic and non-spontaneous. This study showed that water hyacinth leaves are a promising candidate to become a precursor during the synthesis of AC because they can remove both organic and inorganic compounds. Besides dye removal, Riyanto and Prabalaras [25] reported that AC developed from water hyacinth leaves via physical and chemical activations successfully removed heavy metals such as Co(II) with a maximum adsorption capacity 140.725 mg/g. Isotherm and kinetic studies revealed that the Co(II) adsorption by water hyacinth leaves-based AC, multilayer, and chemisorption was predominant. From the results obtained, it can be concluded that water hyacinth leaves based AC can reduce the concentration of heavy metals ions Co(II).

Moosa et al. [26] studied the adsorptive removal of lead ions (Pb^{2+}) using a green adsorbent synthesized from aloe vera leaves. The surface chemistry of adsorbent developed from aloe vera leaves shows the presence of H-bonded acetyl, carboxyl, phenolic, and amine groups. The maximum adsorption efficiency for removing lead ions was 97.29% and 97.28% for non-modified aloe vera AC (2.2 g, pH 5 and 6 hr) and modified aloe vera AC (1.6 g, pH 5 and 6 hr), respectively, at optimum conditions. On the hand, aloe vera leaves can treat toxic aniline, methylene blue (MB), and methyl orange (MO) dyes from aqueous solution with maximum adsorption capacity of 185.18, 129.87, and 196.07, respectively, as reported by Khaniabadi et al. [27]. Similarly, SEM analysis of chemically activated aloe vera AC with H_2SO_4 activation shows a regular porous structure with a larger surface area and subsequently more active sites in the adsorbent surface than non-modified aloe vera AC. These studies show that chemically modified AC of biomass leaves recorded higher surface area and adsorption properties than non-modified material.

On the other hand, Ahmad et al. [28] synthesized AC from lemongrass leaves and chemically activated it with NaOH solution to exclude MB dye. The surface morphology of lemongrass leaves char showed that the pores were not well developed with a rough surface. But the surface morphology of chemically activated lemongrass leaves-based adsorbent revealed that the chemical activation process has resulted in the formation and widening of the AC pore. The enhancement in structure porosity and surface area is advantageous in achieving excellent MB dye adsorption performance Adsorption study showed that lemongrass leaves AC achieved 342.9 mg/g of MB dye adsorption capacity. This study concluded that chemically modified lemongrass leaves AC can perform the MB dye adsorption process better than non-activated lemongrass leaves char. Do et al. [29] also prepared AC from Moringa oleifera

leaves with NaOH activation to treat MB dye. Similarly, the surface morphology showed that un-activated Moringa oleifera leaves have a less porous surface. But the SEM analysis showed that Moringa oleifera leaves AC with chemical activation have a honeycomb structure with large pores on the surface, which leads to a larger surface area for adsorption. The chemically activated Moringa oleifera leaves achieved 136.99 mg/g of MB dye adsorption capacity, the overall process was exothermic, and physisorption was predominant. These studies have proven that chemical activation is significant in developing the porous structure of biomass leaves-based AC to remove recalcitrant pollutants effectively.

Besides leaves, researchers also widely explored fruit peels, which are biodegradable, non-toxic, and abundant to synthesize adsorbents for dye adsorption [30]. For example, Fernandez et al. [31] studied the preparation of AC from orange peel through H_3PO_4 activation to remove MB and Rhodamine B dyes. The surface chemistry of H_3PO_4-treated orange peel AC shows the strong vibrations of H-bonded O-H from phenols or alcohol and carboxyl groups, carboxylate groups and ester groups. They reported that the BET surface areas exhibited by raw orange peel precursor and H_3PO_4-treated orange peel AC were 1.1 m^2/g and 1,090 m^2/g, respectively. Besides, 1.2×10^{-3} and 1.2 cm^3/g of pore volumes were recorded for raw orange peel and H_3PO_4-treated orange peel AC. These results showed a significant porous structure development during the H_3PO_4 treatment, which benefits the MB and Rhodamine B dye adsorption. On the other hand, Dey et al. [32] studied ammonia and nitrate removal by utilizing a biosorbent developed from biomass orange peel. Similarly, the surface chemistry of orange peel biosorbent shows the presence of hydroxyl, carbonyl, amine and aromatic groups, which are crucial in removing ammonia and nitrate molecules from an aqueous solution. They reported that the surface area achieved was up to 45.42 m^2/g, and pore volume of up to 0.512 cm^3/g was exhibited by orange peel biosorbent. These studies showed that hydroxyl and carbonyl groups have a high affinity toward pollutants. Thus, it can be concluded that these significant functional groups contribute to the attraction of pollutants by adsorbents through binding and trapping.

Ahmad et al. [13] studied the development of AC from pomegranate peel using CO_2 gasification and chemically activated with KOH for MB dye adsorption. The surface morphology analysis showed that the raw pomegranate peel had a rough and non-porous surface. But widening and enhancement of pores were identified in modified pomegranate peel AC. The surface area of raw pomegranate peel was 1.01 m^2/g and 845.96 m^2/g for modified pomegranate peel AC. This study showed that modified pomegranate peel AC has a higher porosity than raw peel, thus enhancing the MB dye adsorption. On the other hand, AC developed from pomegranate peel using potassium carbonate (K_2CO_3) as an activating agent able to adsorb CO_2 with a high adsorption capacity (717 mg/g), as stated by Saadi et al. [33]. Based on the surface morphology analysis, the non-modified pomegranate peel was uneven and rough. However, numerous cavities were discovered on the modified pomegranate peel AC's external surface, which increases the porosity of the adsorbent. The BET surface area achieved by modified AC developed from pomegranate peel was up to 1,860 m^2/g.

Moreover, hard shells such as walnut and coconut shells (CS), which are highly degradable, have high regeneration capacity and low cost, have been used for adsorbent preparation. Dahri et al. [34] studied adsorbent preparation from walnut shells to remove malachite green (MG) dye and isotherm; kinetic and thermodynamic studies were investigated. Characterization of walnut shells showed hydrogen (5.63%) and carbon (48.46%) groups, which are important for dye adsorption. The walnut shell successfully removed MG dye with a maximum adsorption capacity of 90.8 mg/g (dosage: 0.03 g/20 mL, pH: 5, agitation rate: 250 rpm, time: 2 h) under optimum conditions. Experimental data on MG dye adsorption revealed that MG dye adsorption is a spontaneous monolayer chemisorption process and endothermic. On the other hand, walnut shells also can remove other dyes, such as MB dye, based on a study reported by Uddin et al. [35]. The elemental analysis showed the existence of carbon (45.93%) and oxygen (54.07%) in the walnut shells, which helped enhance the adsorption property of walnut shells towards MB dye molecules.

Similarly, MB dye adsorption follows a monolayer pattern of the chemisorption process. In addition, the exothermic and spontaneous MB dye adsorption process was also concluded from the study. These studies have proven that walnut shell is a promising biomass material to prepare adsorbents for the removal of recalcitrant pollutants from aqueous solutions.

Oribayo et al. [15] studied the MB dye adsorption using AC developed from CS with zinc chloride ($ZnCl_2$) activation. Based on the surface morphology analysis, the surface of non-activated CS has low porosity. On the other hand, the surface of AC has high porosity after activation of CS. The maximum MB dye adsorption capacity achieved by CSAC was 320.5 mg/g under optimum conditions (pH: 7, dosage: 0.02 g, and contact time: 4.5 h). The isotherm, kinetic and thermodynamic studies revealed that MB dye adsorption by $ZnCl_2$-treated CSAC was spontaneous monolayer chemisorption process and endothermic. On the other hand, Aljeboree et al. [36] stated that CS could treat textile dyes (maximum blue GRL and direct yellow DY 12 dyes) from contaminated solutions. The surface morphology of CSAC was well developed with a significant pore, which enhances the adsorption of textile dyes. Fritz-Schlunder isotherm and pseudo-second-order kinetic model best described the experimental data at equilibrium, which suggested that chemisorption is predominant. The thermodynamic study demonstrated that the textile dye's adsorption was exothermic and spontaneous. The literature revealed that biomass wastes are promising biomaterial for synthesizing biosorbents for recalcitrant wastewater treatment. Modifying the biosorbents greatly affects the surface chemistry and morphology of the structure, which significantly enhances the affinity of biosorbents toward pollutants.

CARBONACEOUS MATERIAL FROM COCONUT SHELL

Coconut trees are abundant in Asia and South America, with a total global production of up to 62.5 million metric tons in 2019. Coconut fruits are processed into different products, including coco fibre, desiccated coconut, cosmochemical, coconut oil, and nata de coco. In 2019, Malaysia ranked as the 10th largest world coconut

producer with a production of 0.54 million metric tons of coconuts [37]. According to the Department of Agriculture of Malaysia (2017), Selangor with the highest production amount of coconut (99,674 tons/year), Johor with the second-highest production amount (95,677 tons/year), followed by the third highest coconut production state, Perak accounted for 87,890 tons/year in the year 2016. However, the high production of coconuts leads to high generation of coconut shell wastes.

CS is composed of lignin, hemicellulose, and cellulose. These components comprise hydroxyl and carboxyl groups that are essential for adsorption [38]. Therefore, CS can be a precursor for producing AC and graphene materials besides being used for handicrafts and as firewood for cooking. Gunawan et al. [39] reported that CS adsorbent obtained a surface area of 220.47 m^2/g with a pore volume of 0.201 cm^3/g. The result of surface area analysis of the CSAC indicated that CS is classified as macropores. Besides, the presence of the C=O indicates that CSAC contains active carbon substances, which help to improve the adsorption performance. On the other hand, Sujiono et al. [40] used CS waste in South Sulawesi province, Indonesia, to produce AC with the aid of different activating agents, including alkaline earth metal salts, phosphoric acid (H_3PO_4), sodium hydroxide (NaOH), and zinc chloride ($ZnCl_2$). The surface area analysis shows that CS with NaOH activation had the highest surface area value (516 m^2/g) compared to other activations. And the total dissolved solids (TDS) measurement showed that AC with NaOH activation meets the requirements for drinking water standards.

Physicochemical characteristics of CS are crucial in assuring the efficiency of converting biomass CS wastes into biosorbents for recalcitrant wastewater treatment. Ahmad et al. [41] reported that CS exhibits a fixed carbon (21.8%), carbon (41%), volatile content (70.8%), ash content (1.8%), low moisture content (5.6%) and high density (412 kg/m^3). They reported that amorphous and crystalline structure was observed in carbonaceous CS. Besides, the surface morphology of CS heterogeneous shapes and pores is well developed with large surface area. These properties make CS an ideal biomass precursor in developing an AC. Biomass materials with low ash content, high carbon content, a considerable amount of volatile content, and high density are preferable to develop an AC. Dongardive et al. [42] reported that the high fixed carbon content in CS contributes to the production of solid residues, which consist of carbon and ash to prepare AC. With the high level of carbon and lignin content, Maniarasu et al. [43] reported that CS could withstand high-temperature changes during the conversion process of CS into adsorbent. It can be concluded that high carbon and lignin content contribute to the high hardness properties of CS.

Additionally, Itodo et al. [44] reported that high CS density helps to enhance the carbon's structural strength to withstand high external pressure onto biomass structure. Finally, Das et al. [45] stated that AC prepared from CS is commonly used to remove toxic pollutants from wastewater because of the development of the pore on the surface of CS, which makes CS have a high affinity toward a wide range of pollutants. These are the properties that justify the potential of CS as the precursor material to develop an effective adsorbent.

SYNTHESIS METHOD OF COCONUT SHELL ACTIVATED CARBON

The synthesis method of AC greatly influences the surface chemistry of adsorbents, including the porous structure and surface area. Therefore, selecting the proper synthesis technique is crucial to enhance the affinity toward a wide range of pollutants. Generally, carbonization and activation are the two fundamental steps for synthesizing coconut shell-activated carbon (CSAC). Carbonization is defined as a slow pyrolysis process where the conversion of biomass wastes into charcoal-like adsorbents with high carbon content occurs under oxygen-free or oxygen-limited conditions [46]. During carbonization, thermal degradation prepares carbonaceous material with enhanced carbon content. Carbonization is controlled by significant parameters, including nitrogen gas flow rate, retention time, temperature, and heating rate. Biochar is the primary product through pyrolysis or gasification at high temperatures under inert conditions. An activation process is required if the developed biochar shows low adsorptive ability. During activation, the activating agent creates a microporous structure with a larger surface area by eliminating disorganized carbon present in carbonaceous material and breaking the walls between the pores. Depending on the type of activation, the activation process can be before or after the carbonization process. Fig. 1 shows the flow diagram for the synthesis of CSAC.

1. Carbonization

1-1. Pyrolysis

Pyrolysis is the thermal decomposition of biomass waste in the furnace in an inert environment to enhance fixed carbon content [47]. During pyrolysis, non-carbon species, including oxygen, nitrogen, and hydrogen, are removed by optimizing the parameters to form well-developed AC. The carbonization temperature affects the process the most, followed by heating, nitrogen gas flow, and retention time. Higher carbonization temperature produces lower yields in biochar with higher carbon and ash content. This phe-

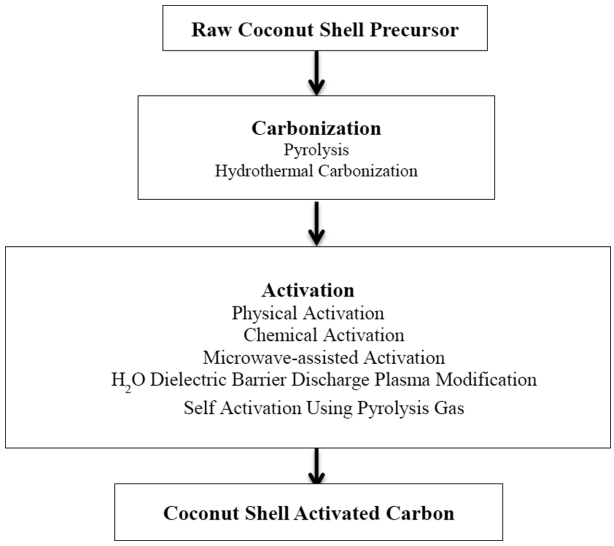

Fig. 1. Flow diagram for synthesis method of coconut shell activated carbon.

nomenon is due to the de-volatilization of biomass and cracking of biochar residue. The pyrolysis method is widely studied in developing an effective adsorbent for wastewater treatment and can be classified into one-step or two-step pyrolysis. One-step pyrolysis is a simultaneous process of carbonization and activation steps without a separate carbonization step and obtains AC directly by pyrolysis [48]. The two-step pyrolysis process includes a separate carbonization step followed by char activation [49]. One-step pyrolysis is more favorable due to lower cost, lower energy consumption, and lower processing time, which meets the requirement from an economic perspective [50].

Table 1 summarizes the adsorbents developed through the carbonization method. In Devens et al. [51], biochar was synthesized from green CS precursors through a pyrolysis process in a muffle

Table 1. Synthesis methods of coconut shell activated carbon

No.	Adsorbent	Synthesis method	Operating conditions	Types of pollutants	Remark	Ref.
1.	CSAC	Pyrolysis	Temp.: 350 °C RT: 1 h	NA	Ash: 33.56±0.41% VC: 29.53±8.77%	[51]
2.	CSAC		Temp.: 300-500 °C	NA	Ash: 1.34-1.53% VC: 71.50-75.93% Pore vol.: 0.15 cm^3/g BET SA: 308 m^2/g	[52]
3.	CSAC		Temp.: 850 °C RT: 60 min Pyrolysis: Single step	NA	BET SA: 1,152 m^2/g	[53]
4.	CSAC/ iron oxide		Carbonization Temp.: 1,000 °C Activation Temp.: 1,000 °C Impregnation ratio (acidic): 125 ml of 20% HNO3 mix with 125 ml of 20% H_2SO_4 Impregnation ratio (base): 1 : 3 (Carbon: KOH) Pyrolysis: Two-step	Oil spill	BET SA: *Acid activation: 580 m^2/g* *Base activation: 1,650 m^2/g* Oil retention capacity: Good	[55]
5.	CS char		Carbonization Temp.: 1,000 °C, 2 h Activation Temp.: 900 °C. 120 min Pyrolysis: Two-step	NA	BET SA: 1,926 m^2/g Total Pore vol.: 1.26 cm^3/g Micropore vol.: 0.931 cm^3/g	[56]
6.	AC of CS+ Municipal Sludge		Single-step pyrolysis: *Temp.: 800 °C,* *RT: 1 h* Two-step pyrolysis: *Carbonization Temp.: 500 °C, 45 min* *Activation Temp.: 800 °C, 1 h* Impregnation ratio: 1 : 1.5 (Mixture: KOH)	MB dye	Single-step pyrolysis: *BET SA: 285.33 m^2/g* *Total pore vol.: 0.35 cm^3/g* *Adsorption capacity: 101.88 mg/g* Two-step pyrolysis: *BET surface area: 683.82 m^2/g* *Total pore vol.: 0.72 cm^3/g* *Adsorption capacity: 602.88 mg/g*	[48]
7.	CSAC hydrochar	Hydrothermal Carbonization	Temp.: 200 °C RT: 2 h Impregnation ratio: 3 : 1 (NaOH : CS hydrochar)	MB dye	Adsorption Type: Monolayer, Chemisorption BET SA: 876.14 m^2/g Adsorption capacity: 200.01 mg/g	[21]
8.	CSAC hydrochar		Temp.: 200 °C RT: 20 h	NA	BET SA: 21.82 m^2/g Pore vol.: 0.09 cm^3/g CC: 58.55 wt%	[59]
9.	CS+Sewage Sludge hydrochar		Temp.: 180 °C RT: 4 h Activation: KOH	MB dye	BET SA: 873.54 m^2/g Adsorption capacity: 172.4 mg/g	[58]
10.	CSAC	Physical activation	Carbonization Temp.: 500 °C Activation Temp.: 850 °C, 60 min Oxidizing agent: CO_2 Physical activation: Single-step	NA	BET SA: 1,152 m^2/g	[53]
11.	CSAC		Activation Temp.: 900 °C, 140 min Oxidizing agent: CO_2 Physical Activation: Single-step	NA	BET SA: 1,667 m^2/g Total pore vol.: 0.8949 cm^3/g	[50]

Table 1. Continued

No.	Adsorbent	Synthesis method	Operating conditions	Types of pollutants	Remark	Ref.
12.	CSAC	Chemical activation (Acidic)	Activation: H_2SO_4	Maxilon Blue GRL dye Direct Yellow 12 dye	Adsorption Type: Multilayer, Chemisorption	[36]
13.	CSAC		Activation: H_2SO_4	MB dye	Adsorption capacity: 50.6 mg/g	[65]
14.	CSAC		Carbonization Temp.: 600 °C Activation: $ZnCl_2$ Impregnation ratio: 1 : 1	MB dye	Adsorption capacity: 320.5 mg/g	[15]
15.	CSAC		Carbonization Temp.: 550 °C Activation: $ZnCl_2$ Impregnation ratio: 1 : 1	MG dye	BET SA: 544.66 m^2/g Adsorption capacity: 19.724 mg/g	[67]
16.	CSAC		Carbonization Temp.: 500 °C, 1 h Activation: $ZnCl_2$ Impregnation ratio: 2 : 1 (char: $ZnCl_2$)	MB dye	BET SA: 935.46 m^2/g Adsorption capacity: 156.25 mg/g	[68]
17.	CSAC		Activation: H_3PO_4 Activation Conc. & Time: 3 M concentration, 9 h	-	Iodine number: 248.5811 mg/g	[69]
18.	CSAC		Activation: H_3PO_4 Activation Conc. and Time: 3 M concentration, 12 h	-	Iodine number: 889.36 mg/g	[70]
19.	CSAC		Activation: NaOH Carbonization Temp.: 500 °C Impregnation ratio: 2 : 1 (NaOH: char)	MB dye	BET SA: 1,842 m^2/g	[73]
20.	CSAC		Activation: KOH Carbonization Temp.: 500 °C Impregnation ratio: 2 : 1 (KOH: char)	Pb^{2+}	BET SA: 1,135 m^2/g	[18]
21.	CSAC	Microwave-assisted Activation	Irradiation power: 500 W Irradiation duration: 5 min	POME	BET SA: 629.43 m^2/g Color removal: 95%	[19]
22.	CSAC		Activation: KOH Irradiation power: 500 W Irradiation duration: 4 min	Benzene & toluene	BET SA: 1,354 m^2/g Removal %: 85%	[74]
23.	CSAC	H_2O Dielectric Barrier Discharge Plasma Modification	Discharge power: 160 W RT: 100 s	NA	BET SA: 846.0 m^2/g Specific capacitance: 84.6%	[75]
24.	CSAC	Self-activation Using Pyrolysis Gas	Temp.: 900 °C RT: 6 h	MB dye	BET SA: 1,194.4 m^2/g Adsorption capacity: 315 mg/g Specific capacitance: 258 F/g Retention rate: 97.2%	[76]

furnace at 350 °C for 1 h without any nitrogen flow and separate activation process. CS biochar was characterized to determine the ash and volatile content. The result revealed that CS biochar exhibited 29.53±8.77% and 33.56±0.41% for volatile and ash content. In addition, they observed micropores, mesopores, and macropores make up the structure of CS biochar. The resulting material also exhibits a honeycomb-like structure of large tubes connected. Similarly, Samsudin et al. [52] developed biochar from CS at self-sustained and low carbonization temperature without any chemical activation. The authors used one-step carbonization of CS at 300-500 °C without any chemical activation process. The CS biochar yield obtained from carbonization was around 30-32%, with 0.15 cm^3/g of pore volume and the BET of 308 m^2/g. Similar to Devens et al., the characterization of CS biochar aimed to observe the effect of temperature on the ash and volatile content [51]. CS biochar developed by Samsudin et al. achieved 71.50-75.93% of volatile content and 1.34-1.53% of ash content [52]. This result justified that CS biochar developed by Samsudin et al. is more desir-

able as an adsorbent for recalcitrant wastewater treatment due to the lower ash content and high volatile content.

On the other hand, Tsai and Jiang [53] developed AC from carbonaceous CS by using one-step pyrolysis, where both the carbonization and activation process happen simultaneously. In their study, dried CS was heated in a tube reactor for 500 °C with heating rate of 10 °C/min. Then when the samples turned to charcoal, activation was done immediately at different temperatures from 700 °C to 900 °C for other holding times (0 min, 5 min, 15 min, 30 min, 45 min, and 60 min). They concluded that activation temperature at 850 °C for 60 min was optimal for obtaining the largest BET-specific surface area (1,152 m^2/g) in AC. On the other hand, Jin et al. [54] reported that a longer activation time leads to a higher activation degree of carbon until the optimum value is achieved.

Additionally, the adsorption performance of the adsorbent increased when the activation temperature increased. However, carbon content may be lost if the activation temperature exceeds the optimum value. The activation temperature and retention time significantly affect the porosity and textural characteristics of developed AC. Besides, the researcher also widely used two-step pyrolysis to synthesize CS-based adsorbents. Raj and Joy [55] used two-step pyrolysis to CSAC/iron oxide composite. CS was first pyrolyzed in a tubular furnace at 1,000 °C with the aid of nitrogen gas flow and then chemically activated with both HNO_3 and H_2SO_4 acid (125 ml of 20% HNO_3 mix with 125 ml of 20% H_2SO_4 at 110 °C for 90 min) and potassium hydroxide (KOH) solution at a ratio of 1 : 3 (carbon: KOH). The acid-treated CS samples were then washed and dried. But for the KOH-treated CS samples, pyrolysis was repeated in the tubular furnace at 1,000 °C under argon gas flow. Lastly, the prepared sample was washed several times to obtain neutral pH before undergoing the drying step in the oven. The samples were then kept in a tightly closed container. The result revealed that the surface areas of KOH-treated CS samples (1,650 m^2/g) are higher than acid-treated CS samples (580 m^2/g). The results obtained from the study revealed that two times pyrolysis before and after the KOH activation helps to enhance the porosity and surface area compared to one-time pyrolysis before activation. Li et al. [56] also used the two-step pyrolysis method to develop carbonized CS char and AC-CS char. Their study aimed to determine how the carbonization temperature affects the pore characteristics of CS char, and AC prepared from CS char at varying temperatures (400, 600, 800, and 1,000 °C) and activation times (30, 60, 90, 120 min). During the adsorbent preparation, the CS samples were heated at different temperatures (400, 600, 800, and 1,000 °C) for 2 h under a nitrogen gas stream with an increment of 10 °C per minute. The samples were crushed and physically heated to different temperatures from 750 °C to 950 °C for every 30 minutes up to 120 minutes. They found that CS samples carbonized at a high temperature of 1,000 °C and physically activated at 900 °C for 120 min achieved the largest surface area (1,926 m^2/g), micropore volume (0.931 cm^3/g), and total volume (1.26 cm^3/g) than other temperature and holding time conditions. Based on the results, the high porosity of adsorbent structure and large surface area of CS char was mainly contributed by higher carbonization temperature and longer retention time.

Yang et al. [48] evaluated the AC prepared by single-step and two-step pyrolysis from the mixture of CS and municipal sludge (MS) for MB dye removal. They carried out one-step pyrolysis after impregnating the mixture of CS and MS with KOH solution at 1 : 1.5 (mixture: KOH) for 24 h. The dried and impregnated mixture was heated in a box-type electric furnace at 800 °C for 1 h, incrementing 40 °C per minute. The samples were then cooled, washed, and dried. They also carried out two-step pyrolysis by adding the carbonization step before the impregnation of the mixture. The steps were the same as one-step pyrolysis, except that Yang et al. pyrolyzed the dried mixture samples in a box-type electric furnace at 500 °C for 45 min in the inert atmosphere before impregnating the mixture with KOH solution [48]. The study shows that AC prepared with the two-step pyrolysis method is more effective with a larger surface area (683.82 m^2/g), adsorption capacity (602.8 mg/g), and total pore volume (0.72 cm^3/g) than single-step pyrolyzed activated carbon (BET surface area=285.33 m^2/g, total pore volume=0.35 cm^3/g, adsorption capacity 101.88 mg/g). Yang et al. revealed that the porous structure of AC developed using the two-step pyrolysis method is well developed and more desirable for adsorption purposes [48]. Compared to the one-step pyrolysis method, the two-step method is more advantageous in developing AC with higher porosity and lower cost. However, single-step pyrolysis is more beneficial economically. By analyzing the previous studies, pyrolysis temperature, retention time, nitrogen gas flow, and heating rate have significant impacts on the structural properties of AC. Furthermore, pyrolysis occurs under high-temperature conditions, where the release of volatile species happens and the increase in fixed carbon content. Thus, a higher pyrolysis temperature prepares a better quality of biochar.

1-2. Hydrothermal Carbonization

The hydrothermal carbonization process (HTC) includes heating biomass precursors at moderate temperatures of 140 °C-350 °C [57]. As a result, solid hydrochar with low ash content, high carbon content, and an abundant amount of oxygen-enriched functional groups will be formed. During HTC, dehydration and polymerization may occur that optimizes the pore structure of the precursor and forms a larger BET surface area in the adsorbent [58]. HTC has several properties, such as it consumes lower energy and time, is eco-friendly, and has higher energy efficiency and chemical reactivity. These properties validate its suitability as an ideal method to produce hydrochar. However, the extensive application of HTC is limited by its poor porosity, small surface area, and low degree of carbonization. Therefore, the chemical activation process is commonly proposed after HTC for the enhancement of surface area and also the development of porous structure [58].

Table 1 summarizes the adsorbents prepared through HTC. Islam et al. [21] developed hydrochar from CS with chemical activation of sodium hydroxide (NaOH) for MB dye removal. Parameters including solution pH and initial MB dye concentration were studied and recorded. During the adsorbent preparation, they carried out a hydrothermal process with 5 g of CS and 100 ml of distilled water at 200 °C for 2 h. The activation process was conducted by impregnating the CS hydrochar with NaOH solution at different ratios of 1 : 1, 2 : 1, and 3 : 1 (NaOH: CS hydrochar) for 4 h. Then, the samples were pyrolyzed in a tubular reactor at 600 °C for 1 h (heating rate: 10 °C/min) under nitrogen flow. They found

that the optimum impregnation ratio of NaOH solution for MB dye adsorption (neutral pH, 30 °C) was at the ratio of 3 : 1 (NaOH: CS hydrochar) with an adsorption capacity of 200.01 mg/g. The NaOH-treated CS hydrochar exhibited a surface area up to 876.14 m^2/g. A monolayer pattern of the chemisorption process on the homogeneous surface could be observed for MB dye adsorption by NaOH-treated CS hydrochar.

Similar to the study by Islam et al., Danso-Boateng et al. [59] conducted HTC at 200 °C but with a longer HTC time (20 h) during adsorbent preparation. Based on the study of Danso-Boateng et al., they developed and analyzed the adsorption characteristics of hydrochar via HTC from different kinds of biomass wastes such as CS, coco-peat, lemon peel, rice husk, and eggshell [59]. The operating conditions were 200 °C for 20 h. After HTC, the carbonized samples were rinsed with methanol followed by deionized water to remove the organic impurities. Finally, the biomass hydrochar was stored at 4 °C for analysis purposes. SEM/EDS, FTIR, and BET analysis characterized the hydrochar developed from CS, coco-peat, lemon peel, rice husk, and eggshells through SEM/EDS, FTIR, and BET analysis. From this study, Danso-Boateng et al. concluded an overall increase in BET surface area of hydrochar for all types of biomass waste after hydrothermal treatment [59]. Among all the biomass wastes, the largest increment in surface area was observed for CS (from 0.71 to 21.820 m^2/g) compared to coco-peat (from 1.23 to 2.14 m^2/g), rice husk (from 0.46 to 15.74 m^2/g), lemon peel (from 0.31 to 6.89 m^2/g), and eggshell (from 0.09 to 0.5 m^2/g). CS exhibited the most significant increment in pore volume after HTC from 0.003 to 0.09 cm^3/g Their analysis showed an increment in carbon content for CS (from 48.07 to 58.55 wt%) but a decrement in H/C (from 0.12 to 0.09 wt%) and O/C (from 0.96 to 0.61 wt%). Therefore, a high degree of aromaticity and oxygen-containing functional groups are favorable for heavy metals adsorption. This study summarized that increasing pores and surface area volume results in more active sites to adsorb contaminants, thus enhancing adsorbents' adsorptive ability. In comparison to Islam et al. [21], CS hydrochar with NaOH activation developed by Islam et al. achieved a higher surface area than biomass wastes-based hydrochars developed by Danso-Boateng et al. This result may be due to NaOH activation's contribution during the hydrochar preparation by Islam et al. Chemical activation is advantageous in developing carbon with higher porosity, which leads to a larger surface area [60].

Tu et al. [58] explored HTC during composite preparation. They aimed to find the best carbonization temperature and time for the highest yield of hydrochar. Different operating conditions, such as activation time and temperature, the concentration of solution, HTC time, temperature, and pH, were investigated. HTC and activation process using sewage sludge (SS) and CS by preparing 8 g of raw material with different impregnation of ratio of SS and CS and 70 mL of deionized water was carried out in the hydrothermal reactor. After obtaining the solid hydrochar, activation of hydrochar with potassium hydroxide (KOH) solutions (1-4 mol/L) was carried out. The mixtures were then pyrolyzed at 300 °C-900 °C for 10-70 min under nitrogen flow (heating rate: 10 °C/min). CS composite with a large surface area (873.54 m^2/g) porous structure was synthesized. The adsorption capacity of 0.6 g/L of SS and CS composite (623.37 mg/g) improved through HTC and activation processes compared to the study of sewage sludge activated carbon (SSAC) (33.47 mg/g) alone investigated by Silva et al. [61]. The optimal hydrothermal condition for best MB dye adsorption capacity (172.41 mg/g) was at pH of 8.5 and the highest hydrochar yield (around 75%) obtained was at temperature of 180 °C and 4 h of HTC time [58]. The carbonaceous material produced with shorter or longer hydrothermal time is not favorable to develop porous structure. The optimal activation temperature for excellent pore formation was at 700 °C for 50 min with 2.5 mol/L of KOH solution. In conclusion, HTC reaction time is crucial in developing adsorbent with highly porous structure. Subsequently, chemical activation helps to enhance pore formation, which justifies the broad applications of HTC and chemical activation in wastewater treatment industries.

By analyzing the results obtained by Islam et al. and Tu et al., the surface area obtained was 876.14 m^2/g and 873.54 m^2/g, respectively. The adsorption capacity obtained by Islam et al. was 200.01 mg/g and 172.41 mg/g by Tu et al. From the results obtained, the BET surface area and adsorption capacity obtained were slightly higher in CS hydrochar developed by Islam et al. This phenomenon was related to where they developed hydrochar through HTC process followed by chemical activation. However, the HTC temperature and duration and the chemical activation agent were different. HTC process temperature was shorter in study of Islam et al. (200 °C, 2 h) compared to Tu et al. (180 °C, 4 h). This study showed that HTC temperature and duration greatly affect the porosity of hydrochar. Moreover, the chemical activating agents used in both studies were different. In conclusion, chemical activating agents have a significant impact in determining the porosity of hydrochar. Till date, very limited studies have been reported on the production of CSAC through HTC. Studies by Islam et al. and Tu et al. involved the HTC process followed by the activation process, but Danso-Boateng et al. only used the HTC process. HTC is more favorable when followed by the activation process because the activation step helps enhance the surface area, structure porosity, and adsorption capacity. From the previous studies discussed above, hydrothermal carbonization usually occurs below 200 °C to produce deep brown solid called hydrochar. Note that researchers did not widely explore the study of HTC on CS precursors.

2. Adsorbent Activation

2-1. Physical Activation

The carbonization process and activation step are essential to enhance the adsorbent structure. Carbonization of raw precursors occurs typically in an inert atmospheric condition. Volatile content in raw precursors can be removed, and fixed carbon can be formed by thermal decomposition. While, the activation process will be carried out after carbonization, aiming to develop a porous network within carbon atoms [62] to form highly carbonaceous material through physical or chemical activation methods [50]. The activating agents, including carbon dioxide (CO_2), air, or water vapor are common physical activators [63]. Physical activation produces a highly developed microporous structure and is two-step activation in general. The carbonization process will be conducted first by pyrolyzing the raw precursor at a temperature below

700 °C and then activation of charcoal formed from carbonization will be carried out at temperature above 700 °C with the aid of oxidizing gas such as CO_2 or steam (H_2O) [53]. Tsai and Jiang [60] used one-step physical activation by carbonizing precursor at 500 °C under nitrogen flow, and activation step was carried out right after the formation of charcoal with the help of oxidizing CO_2 gas at 700 °C-900 °C with an increment of 50 °C using holding time of 0-60 min. The optimal temperature and holding time for activation were 850 °C and 60 min, respectively, for the preparation of CSAC with BET surface area of 1,152 m^2/g. The difference between conventional physical activation method and method studied by Tsai and Jiang [53] is the separation of carbonization from activation step or simultaneous occurrence of activation process right after carbonization.

Yang et al. [50] also used the one-step CO_2 activation method, as shown in Table 1. In their study, CS precursor was heated in a tubular furnace at activation temperature in the range of 750 °C-950 °C for 60 min-160 min, the heating rate at 10, 30, 50 °C/min, and flow rate of CO_2 was set at 60-600 cm^3/min. The study indicated that activation temperature of 900 °C, 200 cm^3/min of CO_2 flow-rate, 10 °C of temperature increase per minute for 140 min were the optimal conditions to achieve maximum BET surface area (1,667 m^2/g) and micropore volume (0.8949 cm^3/g). In conclusion, the pore characteristics of adsorbent are greatly affected by heating rate, CO_2 flow rate, holding time, and activation temperature. CSAC developed by Yang et al. revealed a higher BET of 1,667 m^2/g [50] compared to CSAC developed in the study of Tsai and Jiang with 1,152 m^2/g of the surface area [53]. The results concluded that higher activation temperature and longer holding time help to enhance the adsorbents' pore properties. In summary, porous structure of adsorbent can be developed using physical activation. During physical activation, activation temperature and retention time have significant impacts on the porosity of adsorbent structure. Thus, optimal operating condition for activating temperature and retention time is important in enhancing the performance of adsorbents.

2-2. Chemical Activation

2-2-1. Acidic Modification

Chemical activation generally includes acidic and basic modifications. Acidic treatment helps to develop cross-link within the material structure and therefore forms porous matrix as well as surface oxidation. Introduction of oxygenated (acidic) chemical functional groups onto carbon surface thus enhances the surface's hydrophilic properties to increase the affinity of adsorbent towards anionic pollutants [64]. This is due to the decrease level of mineral in the carbon surface. Chemical activation forms the mesoporous structure and large surface area in AC by causing swelling, dehydration, and condensation interactions with carbon [48]. The utilization of sulfuric acid (H_2SO_4) as an oxidizing activator in acidic treatment is beneficial due to its super oxidative power, ability to enhance surface functionality, and cost [65]. Aljeboree et al. [36] and Jawad et al. [65] studied the H_2SO_4-treated CS-based adsorbent for dye removal applications. Both groups conducted a study on the treatment of cationic dyes by CS-based adsorbent chemically activated with H_2SO_4, but they obtained different results. Based on Table 1, Aljeboree et al. [36] reported that maxilon blue GRL and direct yellow 12 (DY 12) dyes adsorption by H_2SO_4-treated CSAC was favorable at acidic pH of 3. In addition, the uptake of both dyes onto H_2SO_4-treated CSAC conformed to Fritz-Schlunder isotherm model and pseudo-second-order kinetic model, which confirmed the occurrence of multilayer heterogeneous process and limited by chemisorption process. However, Jawad et al. [65] reported that MB dye adsorption by H_2SO_4-treated CS biosorbent was favorable at alkaline pH of 8. Moreover, the adsorption of MB dye was best fitted with Freundlich isotherm model and pseudo-second-order kinetic model with the maximum adsorption capacity of 50.6 mg/g. Similar to the study of Aljeboree et al., a multilayer pattern of MB dye adsorption was observed on the heterogeneous surface and was limited by the chemisorption process too. From the studies investigated by Aljeboree et al. and Jawad et al., all of the three types of dye used in their studies were cationic dyes, but the optimum dye adsorption pH was in different range. It is possible to conclude that adsorption mechanism for dye adsorption not only depends on electrostatic attraction, but also on hydrogen bonding (H-H) and π-π interactions [66].

Besides H_2SO_4, preparation of CSAC was also done via chemical modification by using $ZnCl_2$ to promote the char formation. The potential of $ZnCl_2$-treated CSAC to remove MB dye was explored by Oribayo et al. [15]. The carbonized CS was impregnated with $ZnCl_2$ at ratio of 1 : 1. From the results obtained, $ZnCl_2$ had increased the carbon content in material from 41.185% to 72.04% by removing H and O component from CS precursor. Increase in carbon content provides hardness and thus promotes the suitability of CSAC in removing pollutants from aqueous solution. 320.5 mg/g of adsorption capacity was achieved for MB dye adsorption under optimum conditions (pH: 7, contact time: 4.5 h of contact time and adsorbent dosage: 0.02 g). Oribayo et al. [15] stated that the surface of $ZnCl_2$-treated CSAC surface was rougher and more porous compared to un-activated carbon. It can be concluded that $ZnCl_2$ was successfully incorporated into CSAC and managed to change the structure of adsorbent, which is more beneficial to an effective adsorption process. Based on Piriya et al. [67], carbonization temperature of 550 °C with the aid of nitrogen flow and impregnation of CS-based adsorbent in $ZnCl_2$ solution at ratio of 1 : 1 (precursor: $ZnCl_2$) successfully removed MG dye with adsorption capacity of 19.724 mg/g. In comparison to study by Oribayo et al. [16], the impregnation of CS with $ZnCl_2$ at same ratio of 1 : 1 (precursor: $ZnCl_2$) and carbonized at 600 °C without nitrogen flow successfully removed 320.5 mg MB dye per gram of adsorbent from aqueous solution. Under inert condition, the porosity of adsorbent structure was enhanced [67]. In both studies, the carbonization temperature was just 50 °C difference with the aid of nitrogen flow. It was revealed from the result that, $ZnCl_2$-modified CS-based adsorbent is more suitable in removing MB dye compared to MG dye. In addition, it can be concluded that carbonization temperature may have an impact on the adsorption performance of adsorbent by developing more porous structure in adsorbent.

Piriya et al. reported in their study that CSAC obtained larger surface area of 544.66 m^2/g after acidic treatment with $ZnCl_2$ at ratio of 1 : 1 and carbonized at 550 °C under nitrogen flow compared to un-activated carbon (425 m^2/g). This result could be compared to the study of Yağmur and Kaya [68] in developing $ZnCl_2$-treated

CSAC for MB dye adsorption. According to their study, there was an increment in surface area of CSAC from 3.39 to 935.46 m^2/g after being impregnated with $ZnCl_2$ at ratio of 2 : 1 (char: $ZnCl_2$) and carbonized at 500 °C under nitrogen flow for 1 h. By comparing Piriya et al. and Yağmur and Kaya, it was observed that the carbonization temperature was just 50 °C difference and impregnation ratio of chars: $ZnCl_2$ were different in both studies. In conclusion, large increment of surface area in $ZnCl_2$-treated CSAC developed by Yağmur and Kaya is mainly contributed by impregnation ratio of chars: $ZnCl_2$, which helps to enhance the porosity of adsorbent. Moreover, chemical activation of CS with phosphoric acid (H_3PO_4) also is used to develop AC, widely. Lutfi et al. [69] and Wang et al. [70] have been discussing about the influences of H_3PO_4 concentration and immersion time on the AC developed from CS precursor. From both studies, iodine number was compared and discussed further. Iodine number is very crucial in indicating the adsorptive ability of developed AC [69]. Lutfi et al. discovered that the optimum H_3PO_4 concentration to develop AC was 3 M and immersion time was 9 h. With this condition, iodine number of 248.5811 mg/g was reported. However according to Wang et al., 3 M H_3PO_4 and immersion time of 12 h were the optimum conditions for the development of AC with iodine number of 889.36 mg/g. Although same H_3PO_4 concentration was used in both studies, the resulting iodine numbers were in large difference. The results conclude that the longer the immersion time of CS in H_3PO_4 solution, the larger the iodine number thus leads to better adsorptive ability. Higher degree of iodine adsorption is ascribed to larger surface area and microporous structure. Lutfi et al. supported this statement in their research study [69]. Previous studies clearly showed that the types of acids that were commonly used in acidic treatment are H_2SO_4, $ZnCl_2$, H_3PO_4 [71]. The significant effect of acidic modification on adsorbent could be observed through the changes in porous structure and surface area of adsorbent. In conclusion, acid-modified adsorbent has higher porosity and surface area. Therefore, it is possible to state that acidic modification helps in enhancing the adsorption performance of adsorbent in removing wide range of pollutants.

2-2-2. Alkaline Modification

Alkaline treatment on the AC enhances the adsorption of negatively charge pollutants as it induces the formation of positive charges on the surface [72]. Reagents such as NaOH and KOH solutions are normally used as alkaline activating agent on CS precursor to develop AC. To date, researchers very rarely apply alkaline modification on CS. Cazetta et al. [73] developed CSAC with NaOH activation for MB dye adsorption. The equilibrium experimental data was perfectly described by pseudo-second-order model and Langmuir model. The maximum monolayer adsorption capacity achieved was 916 mg/g. The best impregnation ratio of NaOH activation to develop AC for MB dye adsorption was 3 : 1 (NaOH: char) and carbonization temperature at 500 °C. With this impregnation ratio, the developed CSAC achieved 2,825 m^2/g of surface area. However, if the impregnation ratio of NaOH: char was 2 : 1, the surface area obtained by CSAC was up to 1,842 m^2/g. Since the surface area obtained by CSAC was different according to different impregnation ratios, it can be summarized that the higher NaOH ratio incorporated into adsorbent, the better the adsorption performance. The result of CSAC with impregnation ratio of 2 : 1 (NaOH: char) developed by Cazetta et al. [73] was compared to the result obtained from Song et al. [18] with different chemical activating agent.

Song et al. [18] reported that CS carbon prepared with KOH activation at ratio of 2 : 1 (KOH: sample) and carbonization temperature of 500 °C for Pb^{2+} removal application achieved surface area of 1,135 m^2/g. By analyzing the results from studies of Cazetta et al. and Song et al., it was observed from Table 1 that under condition of same impregnation ratio, higher surface area was obtained in NaOH-modified CSAC compared to KOH-modified CSAC. It can be concluded that KOH and NaOH have different activation mechanism, and NaOH activation helps to develop AC with larger surface area than KOH even with the same impregnation ratio. In conclusion, chemical activation including acidic and alkaline modification helps to enhance the surface area and porosity of adsorbent, thus helps to enhance the adsorptive ability of adsorbent.

2-3. Microwave-assisted Activation

Microwave-assisted activation is the process where heat transfer and uniform distribution is facilitated by interior heat generated from dipole rotation and ionic conduction between char particles, compensating the char activation period and energy consumption. Based on Table 1, Abdulsalam et al. [19] studied the color removal of palm oil mill effluent (POME) using CSAC, which was pre-treated by microwave irradiation at 100 W for 5 min. Result of their study revealed that microwave irradiated CSAC achieved BET surface area up to 629.43 m^2/g. and successfully removed 95% of color from POME at optimum condition (pH: 2, contact time: 5 h and adsorbent dosage: 5 g/100 mL). Langmuir model was the best-fitted to explain the adsorption mechanism, suggesting the color removal process of POME is monolayer on homogeneous surface. In addition, Mohammed et al. [74] also synthesized CSAC using KOH activation and CSAC was pretreated with microwave irradiation for the removal of benzene and toluene. They did microwave heating on CSAC at power of 500 W for 4 min. The result revealed that KOH-treated CSAC under microwave irradiation achieved surface area of 1,354 m^2/g and successfully removed only 85% of benzene and toluene, and Langmuir isotherm was accurately described for adsorption mechanism, which suggested monolayer adsorption on homogeneous surface. The surface area of CSAC developed by Mohammed et al. is higher than that of Abdulsalam et al. This may possibly be due to the contribution of KOH activation, which helps to develop more porous structure in CSAC. Additionally, microwave heating power and duration also may possibly affect the adsorption mechanism of adsorbent.

2-4. H_2O Dielectric Barrier Discharge Plasma Modification

Dielectric barrier discharge plasma method is a process where water (H_2O) plays role as medium to introduce the oxygen containing functional groups without causing any destruction on pore structure of developed adsorbent, and this method has been used rarely used [75]. As stated by Wang et al. [75], AC developed from CS precursor was cleansed with distilled water to get rid of the ash content. Then, the AC was soaked in deionized water for one day, and then it was washed with 1 M of HCl solution. The pH value was then adjusted until pH 7 by using deionized water and AC was dried for 12 hours at 110 °C. The following steps are signifi-

cant about H_2O dielectric barrier discharge plasma method. About 500 mg of AC with thickness of around 1 mm was placed in the reactor chamber for each cycle. Water bath connected beside was used to heat the water and a vacuum pump was connected to maintain the pressure in the reactor chamber at 30 kPa. They reported that larger surface area of 846.0 m^2/g was observed in AC after modification with H_2O plasma compared to unmodified activated carbon with 779.8 m^2/g. Besides, enhancement of hydrophilicity of CSAC surface was observed. The result revealed that electrochemical properties of CSAC could be improved by simple H_2O plasma modification by introducing oxygen functional groups to carbon surface.

2-5. Self-activation Using Pyrolysis Gas

Process of self-activation using pyrolysis gas is carried out in a closed reactor containing CS and the air inside reactor or O_2 adsorbed by biomass wastes can be the activating agents to develop micropores in biochar at autogenerated pressure condition [76]. Till now, the study of self-activation method on CS-based adsorbent has been limited. However, this method has been studied to develop microporous CSAC to enhance the performance of electric double layer. Sun et al. [76] conducted self-activation experiment by setting up an autoclave to keep the autogenerated pressure during self-activation process. They reported that the autoclave reactor must be sealed all the time because large amounts of pyrolysis gases were generated, thus generating autogenerated pressure under very high temperature (700-1,000 °C). The self-activated CSAC at 900 °C for 6 h obtained a surface area of 1,194.4 m^2/g and MB dye adsorption capacity of 315 mg/g. Moreover, AC achieved 258 F/g of specific capacitance and retention rate of 97.2% even after 3,000 cycles.

PREPARATION METHODS OF HYBRID COCONUT SHELL ACTIVATED CARBON

1. Impregnation

Impregnation is a process where other composite materials are loaded on the carbon surface to enhance adsorption performance of adsorbent [73]. Table 2 summarizes the recent studies on the various impregnation methods used for the development of AC from CS precursor. Van et al. [77] developed CSAC loaded with silver nanoparticles (AgNPs) for the removal of MB dye from aqueous solution. AgNPs were loaded on AC through incipient wet-impregnation technique, where AC surface was contacted with solution containing AgNPs. Different impregnation ratios ranging from 0-1.5% w/w of AgNPs and AC were carried out, but the result showed that the best impregnation ratio was 0.5% w/w. In addition, 172.22 mg/g of maximum adsorption capacity of was achieved under conditions of pH 10, 120 min of contact time and 250 mg/25 mL of adsorbent dosage. Sips model, pseudo-first and pseudo-second kinetic models described the adsorption of MB dye very well. Besides AgNPs, Prajapati and Mondal [78] investigated the effect of loading of copper oxide nanoparticles (CuO-NPs) on nanoporous AC for MB dye removal. The result revealed that the maximum adsorption of MB dyes occurred at pH 9 within 180 min. Successful impregnation of CuO-NPs on CSAC successfully

Table 2. Preparation methods of hybrid coconut shell activated carbon

No.	Adsorbent	Synthesis method	Operating conditions	Types of pollutants	Remark	Ref.
1.	CSAC	Impregnation	Loading particle: AgNPs Impregnation ratio: 0.5% w/w	MB dye	Adsorption capacity: 172.22 mg/g	[77]
2.	CSAC		Loading particle: CuO-NPs	MB dye	Adsorption capacity: 464.2 mg/g	[78]
3.	CSAC/ $CoFe_2O_4$		Temp.: 700 °C RT: 3 h Impregnation ratio: 1 : 2 : 200 (Cobalt : iron : CSAC) Pyrolysis: Single step	Rhodamine B dye	Adsorption capacity: 94.08 mg/g	[16]
4.	Fe_3O_4/ AC/TiO_2		Temp.: 800 °C RT: 2 h Impregnation ratio: 1 : 2 (Fe_3O_4/AC: TiO_2) Pyrolysis: Single step	MB dye	Degradation rate: 98%	[82]
5.	CSAC/ iron oxide	In-situ Co-Precipitation	Impregnation ratio: 1 : 1	Oil spills	Oil retention capacity: Good	[55]
6.	CSAC/ iron oxide		Fenton reagent: H_2O_2 Loading %: 2%	MB dye	Adsorption capacity: 85.45%	[79]
7.	CAC/$CoFe_2O_4$	Single-step Refluxing Router	Impregnation ratio: 1 : 2 : 200 (Co : Fe : CAC)	Rhodamine B dye	Adsorption capacity: 94.08 mg/g	[16]
8.	AC/$CoFe_2O_4$		Immersion solution: NaOH	MG dye	Adsorption capacity: 89.29 mg/g	[80]
9.	AC/$CoFe_2O_4$		Immersion solution: NaOH	GV dye	Adsorption capacity: 184.2 mg/g	[81]

removed 464.2 mg of MB dye per 1 g of CSAC loaded with CuO-NPs at 318 K. The uptake of MB dye onto CSAC loaded with CuO-NPs was best presented by Sips model and pseudo-second order kinetic model, where the MB dye adsorption could be any one of monolayer or multilayer and is limited by chemisorption process. Moreover, CSAC/CuO-NPs composite obtained high desorption rate (93.51%) with 0.1 M HCl solutions. Therefore, it can be justified that CuO impregnated AC developed from CS is an excellent choice to be utilized as adsorbent.

The result revealed that CSAC/CuO-NPs composite synthesized by Prajapati and Mondal achieved higher adsorption capacity [78]. The doping of CuO-NPs enhances the adsorptive ability of CSAC. The result revealed that larger amount of dyes can be adsorbed when contact time increases. Therefore, it can be concluded that loading of CuO-NPs and contact time play a significant role in MB dye adsorption. To date, only few researchers have studied the impregnation on CS-based adsorbent.

2. In-situ Co-precipitation

In-situ co-precipitation is widely used to prepare magnetite particles such as iron oxide nanoparticles. Raj and Joy [55] prepared CSAC/iron oxide nanocomposite through in-situ co-precipitation method for removing oil spills. The weight ratio of AC developed from CS to iron oxide was fixed at 1 : 1. Result showed that CSAC/iron oxide composite is a high potential adsorbent with good oil retention capacity. In-situ co-precipitation method was also studied by Amelia et al. [79] for developing magnetic CSAC for MB dye degradation with the aid of Fenton reagent (H_2O_2). Amelia et al. [79] loaded different impregnation amounts (0.5%, 1% and 2%) of iron on CSAC during the adsorbent preparation. As a result, they found that loading of iron on CSAC at 2% achieved the highest MB dye adsorption capacity (85.45%) compared to loading amount of 0.5% (79.98%) and 1% (83.85%), respectively, without Fenton reaction. With the presence of Fenton reaction, reduction of MB dye concentration from 20 ppm to 4 ppm within 180 min was observed. On the contrary, reduction from 20 ppm to 7 ppm in MB dye concentration was observed within 180 min. Significant reduction of MB dye in the presence of Fenton reagent was mainly caused by the simultaneous occurrence of degradation and adsorption processes. Degradation of MB dye was contributed by the reaction between hydroxyl radicals obtained from H_2O_2 and iron particles. Therefore, it can be concluded from Table 2 that higher loading percentage of iron on CS-based adsorbent leads to more effective and fast catalytic reaction, which brings to higher adsorption capacity. It was found that MB dye adsorption and degradation are more effective with the addition of Fenton reagent. In conclusion, the presence of Fenton reagent and loading amount of iron plays a significant role in determining the effectiveness of catalytic reaction.

3. Single-step Refluxing Router

Single-step refluxing router method was also used by some researchers to synthesize CS-based adsorbents for dye removal application. NaOH solution was diluted in distilled water and stirred for half an hour at room temperature before CSAC was added into solution to obtain AC suspension. Hoang et al. [16] developed coconut activated carbon/cobalt ferrite (CAC/$CoFe_2O_4$) composite for the exclusion of Rhodamine B dye from aqueous solution. The composition of CAC was calibrated with different molar ratios of cobalt: iron: coconut activated carbon (Co : Fe : CAC) at 1 : 2 : 300, 1 : 2 : 250, 1 : 2 : 200, 1 : 2 : 150 and 1 : 2 : 100. Hoang et al. found that the molar ratio of Co : Fe : CAC at 1 : 2 : 200 was the best condition to adsorb Rhodamine B dye with the highest adsorption capacity of 94.08 mg/g under optimum conditions (pH 4, 0.05 g/25 mL of adsorbent dosage and 350 mg/L of initial concentration). The chemisorption process of Rhodamine B dye by CAC/$CoFe_2O_4$ composite was contributed by hydrogen bonding, electrostatic attraction and π-π interactions based on their result. The single-step refluxing router method was also used by Ai et al. [80] in synthesizing AC/$CoFe_2O_4$ adsorbent to adsorb Malachite Green (MG) dye (adsorption capacity: 89.29 mg/g) and Liang et al. [81] in preparing magnetic AC/$CoFe_2O_4$ composite to adsorb Gentian Violet (GV) dye (adsorption capacity: 184.2 mg/g). From these studies, the remarkable results of adsorption capacity have proven that $CoFe_2O_4$ was successfully incorporated onto AC and has justified the potential of single-step refluxing router method in synthesizing adsorbent.

PROPERTIES OF COCONUT SHELL ADSORBENT

Applications of adsorbents prepared from CS have gained significant interest recently in wastewater treatment, as biomass CS are beneficial in terms of long-term sustainability and cost-effectiveness [72]. However, the performance of adsorbents in terms of adsorption capacity and removal efficiency could be enhanced further by modifications. Therefore, a suitable activation process is required to target the precursors' structure to enhance adsorbent reactivity towards pollutants. Factors including porosity and surface functional groups affect the adsorption performance of AC in terms of color removal efficiency, adsorption capacity, COD removal, etc. Modifying surface functional groups according to suitability is crucial in determining adsorbent characteristics, whether acidic, basic, or neutral [83]. For instance, acidic treatment introduces a more considerable amount of oxygenated functional groups in material, which causes oxidation and increases the acidic property of adsorbent [72]. The characterization of adsorbents mainly was focused on the changes in pore size, specific surface area, and micropore volume. Fourier transform infrared spectroscopy (FTIR), scanning electron microscopy/energy dispersive spectroscopy (SEM/EDS) and Brunauer-Emmett-Teller (BET) surface analyzer have been used to study the surface chemistry and morphology before and after the adsorption process. FTIR was used to present the surface functional groups of modified and unmodified adsorbents. SEM/EDS shows the surface morphology and elemental composition of AC. The number of pores present in the AC can determine the porosity of the adsorbent structure. In addition, EDS confirms any addition or increment in the percentage of components in the adsorbent structure after modification. BET surface analyzer presents the changes in specific surface area of adsorbents before and after modification and adsorption process.

Das et al. [45] studied the difference between raw CS precursor and CSAC by comparing their structure and characteristics. The result reported that raw CS precursor has certain limitations compared to modified CS, such as carbon content, micropore volume,

ash content, and BET specific surface area. In the case of raw precursor, the study revealed that raw CS precursor has a lower BET surface area (59.728 m^2/g) than CSAC (995.799 m^2/g). This result indicates that CSAC has better adsorption performance as it can adsorb more contaminants with larger surface area. In contrast, raw CS precursor's low specific surface area limits the adsorptive ability to remove pollutants from wastewater. Besides, the ash content of raw CS and CSAC was determined to be 2.564% and 0.902%, respectively, which shows that CSAC is an excellent choice for adsorbent development. Dongardive et al. [42] supported this statement by saying that precursor with lower ash content is more suitable to develop adsorbents. CSAC is a more effective adsorbent than raw CS precursor because adsorbent with larger micropore volumes can adsorb more pollutants. Besides these characteristics, Das et al. also reported that raw precursor has lower carbon content (41.185%) than CSAC (72.04%). High carbon content in CSAC justifies its potential as a promising candidate to treat dyes in the future compared to raw CS due to its strong withstand ability under high-temperature conditions during adsorption or conversion. The modified CSAC achieved higher removal efficiency of MB dye (~85%) than raw CS, which only reached around 68% by using 4 gm of adsorbents.

Tan et al. [72] studied non-modified and modified CSAC by analyzing CSAC, CSAC treated with 1 M HCl, and CSAC treated with 1 M NaOH. The analysis result showed an increment in micropore volume, BET specific surface area, average pore diameter, and total pore volume in 1 M HCl treated AC compared to untreated AC. 525 m^2/g, 0.272 cm^3/g, and 0.291 cm^3/g were achieved by 1M HCl treated AC for BET surface area, micropore volume, and total pore volume. However, the result showed that untreated AC only performed 436 m^2/g, 0.218 cm^3/g, and 0.229 cm^3/g of BET surface area, micropore volume, and total pore volume. The results concluded that acidic treatment on the AC helps to improve the hydrophilic nature of the surface by increasing the acidity property of the carbon surface, thus changing the pore structure and chemical properties of the adsorbent. But, unfortunately, according to Tan et al. [72], decrement in BET surface area (from 436 to 346 m^2/g), micropore volume (from 0.218 to 0.186 cm^3/g) and total pore volume (from 0.229 to 0.199 cm^3/g) was observed when treating AC with 1 M of NaOH. The assumption was that blockage of pores by oxygen-containing functional groups happened during acidic treatment. Thus, a decrease in surface area is highly associated with a reduction in pore volume. In summary, the analysis results indicated that the acidic and alkaline treatment could alter the surface morphology and properties of AC that can affect their adsorption capacity. Through acidic and alkaline treatment, surface area and porosity of adsorbent will be enhanced due to formation of cross-link, which helps to increase the affinity of adsorbent towards pollutants.

Table 3 summarizes different types of modifications on AC developed from carbonaceous CS and results of BET surface area of non-pretreated and pre-treated AC. Raj and Joy [55] developed CSAC/iron oxide composite and compared the non-pretreated and pre-treated composite with KOH. CSAC/iron oxide composite activated with KOH at the ratio of 1 : 3 (carbon: KOH) achieved a larger surface area (1,650 m^2/g) than non-modified composite (580 m^2/g). It is advantageous to use higher weight ratio of KOH : carbon because a wider pore diameter could be formed (up to 25 Å) from

Table 3. Modifications of coconut shell activated carbon

No	Type of modifications	BET surface area (m^2/g)	Ref.
Impregnation of iron oxide+base treatment			
1	CSAC-iron oxide	580	[55]
2	CSAC-iron oxide (1 : 3 carbon to KOH)	1,650	[55]
Microwave radiation			
3	Raw CSAC	562.5786	[19]
4	CSAC-microwave radiation (pre-treated)	629.4341	[19]
$CoFe_2O_4$ loading			
5	CSAC	867.449	[16]
6	CSAC-$CoFe_2O_4$	759.638	[16]
CuONPs loading			
7	CSAC	387.48	[78]
8	CSAC-CuONPs	262.35	[78]
Impregnation of iron oxide+acidic treatment			
9	CSAC (activated with $ZnCl_2$)	935.46	[68]
10	Magnetic AC (activated with $ZnCl_2$)	747.71	[68]
AgNPs loading			
11	CSAC	691.64	[77]
12	CSAC-AgNPs	705.32	[77]

the fusion of micropores compared to non-pretreated composite (up to 14 Å). Romanos et al. [84] supported this statement by concluding that the amount of potassium material incorporated into carbon matrix increased by increasing the weight ratio of KOH : carbon and resulted in enlargement of pores and increase in porosity. The statement made by Romanos et al. is in line with the result that adsorbent pre-treated with KOH in the ratio of 1 : 3 has higher surface area than non-pretreated CSAC. These results conclude that porosity is highly dependent on the weight ratio of the carbon: activating agent.

Abdulsalam et al. [19] also identified a similar trend for microwave irradiation treatment on CSAC. By comparing non-pretreated and pretreated CSAC, they observed an increase in surface area from 562.5786 to 629.4341 m^2/g after pre-treated CSAC with microwave irradiation. This phenomenon was due to the oxidation process that produced volatile compounds and led to porous structure formation on the carbon surface. In conclusion, the larger the pore volume, the larger the total micropore volume, ascribed to the increment in surface area. Besides studies of Raj and Joy and Abdusalam et al., Van et al. [77] also discovered an increment of surface area after loading of metal materials on CSAC. According to the result obtained, a small increment of surface area from 691.64 to 705.32 m^2/g after impregnating AC with AgNPs indicated the successful incorporation of AgNPs onto AC. Even though there was only a slight increment of surface area, a noticeable increment in maximum adsorption capacity of CSAC-AgNPs (84.81 mg/g) compared to AC (38.89 mg/g) without loading of any particles was observed. In conclusion, adsorbent with a larger surface area has better adsorption capacity.

Hoang et al. [16], Prajapati and Mondal [78], and Yağmur and Kaya [68] reported that BET surface area was observed to be decreased after loading other composite materials onto the AC. CSAC loaded with $CoFe_2O_4$ by Hoang et al. and the BET surface area shows slight decreases compared to unloaded AC from 867.449 to 759.638 m^2/g, and average pore volume was also affected and experienced reduction from 0.381 to 0.321 cm^3/g [16]. This phenomenon was due to the successful deposition of $CoFe_2O_4$ and managed to cover the carbon surface. In addition, Hoang et al. reported that elements such as Co, Fe, and O after the loading process had proven the successful deposit of $CoFe_2O_4$. However, the surface area was still significant even after loading $CoFe_2O_4$ particles on AC. Prajapati and Mondal observed a similar trend when loading CuO-NPs onto the AC. They reported that there was a reduction in surface area from 387.48 to 262.35 m^2/g after loading CuO-NPs onto the AC. This phenomenon was due to the pores being filled by the deposition of CuO-NPs on the surface. It is possible to conclude that a decrease in pore volume causes a decrease in BET surface area. Moreover, Yağmur and Kaya reported a reduction in surface area from 935.46 to 747.71 m^2/g when impregnating iron onto CSAC [68]. This phenomenon also indicated the successful loading of iron oxide on the porous structure of AC. The previous studies summarized that deposition or loading of other composite materials onto CS-based adsorbent changes the characteristic of adsorbent in terms of porosity and surface area.

APPLICATION OF COCONUT SHELL BASED ADSORBENT FOR POLLUTANT REMOVAL

Table 4 summarizes the recent studies on the role of CS adsorbents in removing pollutants from wastewater, including dyes, heavy

Table 4. Applications of coconut shell-based adsorbent for pollutants removal

No.	Adsorbent	Operating conditions	Types of pollutants	Remark	Ref.
Dyes					
1.	CSAC	pH: 12 RT: 50 min Temp: 353.15 K Initial dye conc.: 10 mg/L	Reactive Blue19 dye	Changes in enthalpy: 7.771 kJ/mol Changes in entropy: 0.035 kJ/mol K Activation energy: 57.84 kJ/mol Isotherm: Langmuir & Freundlich Kinetic: P-S-O	[86]
2.	CS charcoal	pH: 11 Adsorbent size: 500-710 μm Initial conc.: 100 mg/L	Basic Yellow 13 dye Basic Red 14 dye	Removal efficiency: 23.6% & 55.7% Adsorption capacity: 19.76 mg/g & 22.93 mg/g Isotherm: Langmuir	[87]
3.	CSAC	pH: 3 Adsorbent dosage: 0.005 g Particle size: 50 μm Temp.: 10 °C Activation: H_2SO_4	Maxilon Blue GRL Direct Yellow 12	Isotherm: Fritz-Schlunder Kinetic: Chemisorption	[36]
4.	CSAC-AgNPs	pH: 10 Impregnation ratio: 0.5% w/w Initial dye conc.: 500 mg/L RT: 120 min Adsorbent dosage: 250 mg/25 mL	MB dye	Adsorption capacity: 172.22 mg/g Isotherm: Sips Kinetic: P-F-O & P-S-O	[77]

Table 4. Continued

No.	Adsorbent	Operating conditions	Types of pollutants	Remark	Ref.
Dyes					
5.	CSAC	pH: 8 Temp.: 700 °C RT: 60 min Adsorbent dosage: 0.1 g Activation: Physical	MB dye	Adsorption %: 99.42% Adsorption capacity: 15.553 mg/g Isotherm: Freundlich Kinetic: P-S-O	[85]
6.	CSAC	pH: 8 RT: 40 min Adsorbent dosage: 0.1 g Activation: H_3PO_4	MB dye	Adsorption %: 98.64% Adsorption capacity: 15.478 mg/g Isotherm: Freundlich Kinetic: P-S-O	[85]
7.	CSAC-CuO-NPAC	pH: 9 Temp.: 318 K RT: 180 min Activation: Physical Adsorbent dosage: 3 g/L	MB dye	BET SA: 262.35 m^2/g Adsorption capacity: 464.2 mg/g Isotherm: Sips	[78]
8.	Iron Oxide-CSAC-Titanium Oxide	Optimum pH: 12 RT: 60 min Impregnation ratio: 1 : 2 (Fe_3O_4 /AC/TiO_2)	MB dye	Degradation rate: 98%	[82]
9.	CSAC-$CoFe_2O_4$	Optimum pH: 4 Initial conc.: 350 mg/L Adsorbent dosage: 0.05 mg/25 mL RT: 150 min	Rhodamine B dye	BET SA: 759.638 m^2/g Pore vol.: 0.321 cm^3/g Adsorption capacity: 94.08 mg/g Isotherm: Freundlich	[16]
10.	CSAC	pH: 7 Adsorbent dosage: 0.02 g RT: 4.5 h	MB dye	Adsorption capacity: 320.5 mg/g Isotherm: Langmuir Kinetic: P-S-O	[15]
11.	Magnetic CSAC	Activation: $ZnCl_2$ Impregnation ratio: 1 : 2 ($ZnCl_2$: Chars) Magnetization: Fe^{2+}/Fe^{3+}	MB dye	Adsorption capacity: 156.25 mg/g Isotherm: Freundlich	[68]
12.	CSCA-$Zn(OH)_2$	Optimum pH: 7 Temp.: 318 K Adsorbent dosage: 0.1 g/100 mL RT: 60 min Initial dye conc.: 100 mg/L	MG dye	Adsorption capacity: 303.03 mg/g Isotherm: Langmuir Kinetic: P-S-O	[88]
Heavy metals					
13.	CS Carbon	pH: 5 Adsorbent Dosage: 4 g/L RT: 2 h Activation: KOH Impregnation ratio: 2 : 1 (KOH: sample)	Pb^{2+}	BET SA: 1,135 m^2/g Pore vol.: 0.442 cm^3/g Adsorption capacity: 151.52 mg/g Isotherm: Freundlich & Halsey Kinetic: P-S-O	[18]
14.	CS Active Charcoal with Chitosan	Optimum pH: 4	Cr (VI)	Removal %: 99.19% BOD: 99.95% COD: 99.825%	[89]
15.	CS	Optimum pH: 2 Activation: steam	Cr (VI)	BET SA: 610 m^2/g Adsorption capacity: ~26 mg/g Isotherm: Langmuir Kinetic: P-S-O	[90]

Table 4. Continued

No.	Adsorbent	Operating conditions	Types of pollutants	Remark	Ref.
Heavy metals					
16.	CS-based Charcoal	pH: 5 Adsorbent dosage: 10 g/L Initial conc.: 2 ppm	Copper	Removal %: 70%	[91]
17.	CSF/Mg-Al composite oxide	pH: 6 Temp: 45 °C RT: 2 h Optimum dosage: 25 mg Initial conc.: 100 mg/L	Phosphorus	BET SA: 38.97 m^2/g Pore vol.: 2.45 nm Adsorption capacity: 60.39 mg/g Isotherm: Langmuir Kinetic: P-S-O	[92]
Other chemical compounds					
18.	CSAC-Iron Oxide	Activation: KOH Impregnation ratio: 1 : 3 (carbon: KOH)	Oil Spill	Surface area: 1,650 m^2/g	[55]
19.	Thermo-Chemical Activated CS	pH: 2 Temp.: 293 K Adsorbent dosage: 3 g/L Activation: H_3PO_4	Sodium Dodecyl Benzene Sulfonate	Adsorption capacity: 28.57 mg/g Isotherm: Langmuir Kinetic: P-S-O	[17]
20.	Coconut Coir AC	Temp.: 304 K RT: 105 min Agitation speed: 100 rpm Activation: KOH Impregnation ratio: 2 : 1 (carbon: KOH)	Oil Spill	BET SA: 691.8 m^2/g Adsorption capacity: 4,859.5 mg/g Isotherm: Freundlich Kinetic: P-S-O	[93]
21.	CS-modified Biochar	pH: 7 Adsorbent dosage: 2.0 g/L Activation: H_3PO_4	Diazinon Pesticide	BET SA: 508.072 m^2/g Pore vol.: 0.146 cm^3/g Adsorption capacity: 10.33 mg/g Isotherm: Langmuir	[94]
22.	Activated Coconut Charcoal	Optimum pH: 7 RT: 60 min	Organophosphorus Pesticide Monocrotophos	BET SA: 79.4 m^2/g Adsorption capacity: 103.9 mg/g Isotherm: Langmuir	[95]

metals, and other organic compounds. The adsorption mechanism of CS-based adsorbents on pollutants was studied and the possible interactions between adsorbents and pollutants were classified into hydrogen bonding, electrostatic attraction and π-π interaction, as shown in Fig. 2. The adsorption process of pollutants is contributed by hydrogen-bonding interactions between N atom in the structure of pollutants and H atom on the surface of adsorbent. Electrostatic attraction is also involved in the adsorption process, where the interactionsare between opposite charges in pollutants and adsorbent surface. Besides hydrogen bonding and electrostatic attraction, π-π interaction also assists in adsorption through π-π electron coupling.

As shown in Table 4, MB dye is the most common cationic dye model used in researchers' studies. Oribayo et al. [15] and Khuluk et al. [85] developed CSAC to treat MB dye. Khuluk et al. physically activated the CSAC by heating the CS precursor in a furnace up to 700 °C and chemically activated using H_3PO_4. Oribayo et al. reported that CSAC without any activation successfully removed 320.5 mg/g of MB dye at optimum conditions (pH: 7, adsorbent dosage: 0.02 g, and contact time: 4.5 h) [15]. The uptake of MB dye was ascribed to the monolayer chemisorption process on a homogeneous surface. However, Khuluk et al. reported that CSAC with physical activation successfully removed 99.42% (~15.553 mg/g) of MB dye at pH 8 and 0.1 g of adsorbent dosage within 60 min [85]. In addition, Khuluk et al. reported that CSAC with H_3PO_4 activation managed to remove 98.64% (~15.478 mg/g) of MB dye at pH 8 and 0.1 g of adsorbent dosage within 40 min. Adsorption isotherm and kinetic studies revealed that MB dye adsorption is a multilayer chemisorption process on a heterogeneous surface. Based on the results obtained by Oribayo et al. and Khuluk et al., removal of MB dye was ideal at pH 7 or greater than 7, which cationic character of MB dye could explain. Moreover, the study revealed that almost complete MB removal percentage was achieved by physically and chemically activated CSAC in a shorter duration compared to non-modified CSAC synthesized by Oribayo et al. This phenomenon could be related to the usage of higher adsorbent dosage and modification done on CSAC, which enhances the adsorptive ability of MB dye. Although a smaller

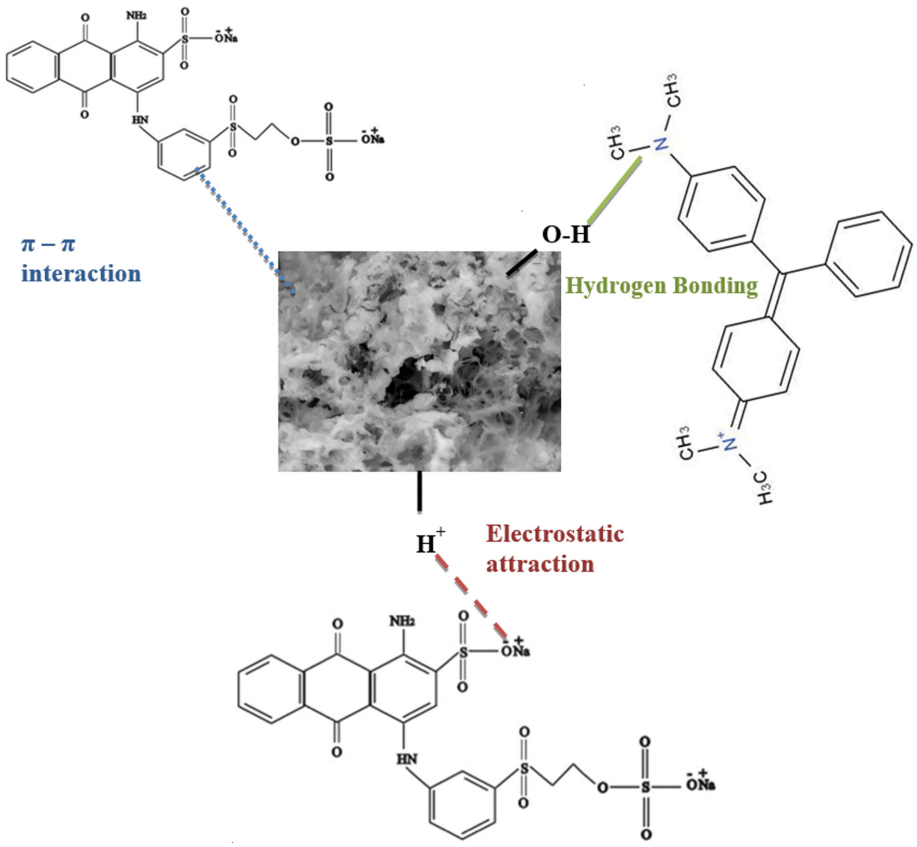

Fig. 2. Adsorption mechanism.

adsorbent dosage is needed to remove MB dye in the study of Oribayo et al., the contact time required was up 4.5h. In conclusion, modification is significant to determine the efficacy of adsorbents in removing a wide range of pollutants.

Besides chemical and physical activation, the mixture of AC with metal oxide composite materials also has gained attention in wastewater treatment. Magnetic adsorbent has been investigated by Prajapati and Mondal [78], Moosavi et al. [82], and Yağmur and Kaya [68] for the case of loading different metallic components such as copper oxide, titanium oxide, and iron oxide onto the activated carbon. The incorporation of iron oxide onto AC helps to improve the catalytic activity of adsorbent and prevents the particles from agglomerating. The magnetic adsorbent is ideal due to the ease of separation and high catalytic activity [96].

Moosavi et al. [82] loaded iron oxide and titanium dioxide on the AC (Fe_3O_4/AC/TiO_2) for degradation of MB dye to determine the adsorption performance and photocatalytic activity of the adsorbent. As stated by Moosavi et al., modification of carbonaceous material such as AC with titanium dioxide and magnetic particles improved photocatalytic activity and reusability properties [82]. Moreover, limitations of titanium dioxide could be overcame by the AC because AC can cause fast charge separation and can accept electrons generated by titanium dioxide, as stated by Moosavi et al. The mixture of AC/iron oxide composite with titanium dioxide is significant in increasing the surface area, enlarging the adsorption area of titanium dioxide, and improving the stability of photocatalyst during regeneration process. Even after seven successive regeneration cycles, Fe_3O_4/AC/TiO_2 catalyst still maintains high efficiency, with only 5% of reduction in photo-activity. The result shows an increment in carbon's size from 50.22 to 62.342 nm when the ratio of AC/iron oxide:titanium dioxide increased from 1 : 1 to 1 : 2. However, particle size decreased when the titanium dioxide ratio increased from 50.22 nm to 45.31 nm when ratio increased from 1 : 2 to 1 : 4. This result showed that aggregation of titanium dioxide might occur on the AC rather than covering it. In conclusion, stable photocatalyst regeneration proves that loading titanium dioxide on AC/iron oxide composite is an effective method to synthesize hybrid CSAC for wastewater treatment.

Prajapati and Mondal [78] also studied the incorporation of metal oxide on AC by loading copper oxide nanoparticles (CuO-NPs) on the CSAC with physical activation. The binding of copper oxides on AC has gained interest for dye degradation because CuO-NPs can bind to the surface of AC through copper and oxygen reactive centers. BET surface area analysis' result confirmed the successful binding of copper oxide onto AC. Prajapati and Mondal [78] reported that there was a reduction in surface area for copper oxide loaded-AC (262.35 m^2/g) compared to AC alone (387.48 m^2/g). The SEM analysis result indicated that only a small number of unoccupied pores were present in the MB dye treated AC. This phenomenon indicates that copper oxide-loaded AC has successfully removed MB dye by filling up most of the pores in the adsorbent. Moreover, the shifting and reduction of peaks for

copper oxide loaded AC composite after MB adsorption was because functional groups present in the AC composite are reacting during the adsorption process.

Besides wide applications in dye removal, CS-based adsorbents also have been used in removing heavy metals from aqueous solution. The utilization of biomass material and metal oxide composite mixture has gained interest in industrial wastewater treatment applications. A study of utilizing coconut shell fibre/magnesium-aluminium (CSF/Mg-Al) as adsorbent has been conducted by Yuan et al. [92] in removing phosphorus from wastewater. Yuan et al. studied the adsorption process of phosphorus via physical and chemical adsorption. The weak bonds between CSF/Mg-Al laminates and interlamellar anions can easily break down to form a new bond leading to the combination of phosphate, magnesium oxide, and aluminum oxide. Besides, an electrostatic attraction forms a bond between the positively charged surface of CSF/Mg-Al and negatively charged phosphate ions. As a result, chemical adsorption occurs between adsorbent and pollutant particles. This phenomenon indicates that the synergistic effect between CSF biomass, magnesium oxide, and aluminum has achieved excellent physical and chemical adsorption of phosphorus from wastewater. In addition, Yuan et al. studied the adsorptive and recycle ability of CSF/Mg-Al composite to remove actual domestic sewage [92]. The result showed that CSF/Mg-Al material has excellent adsorption (60.39 mg/g) and recycling performance than the commercial AC. About 46% of the average removal rate still can be reached even after three times of recycling process compared to the commercial AC (28%). In summary, CSF/Mg-Al adsorbent is a promising candidate to remove total phosphorus from wastewater in the future.

Other than dyes and heavy metals, focusing on removing other chemical compounds has gained significant interest. Raj and Joy [55] investigated the ability of CSAC-iron oxide magnetic adsorbent with KOH activation to remove oil spills (carbonization temp: 1,000 °C, activation temp: 1,000 °C). Raj and Joy reported that activation of CS-based adsorbent with a high carbon: KOH ratio (1 : 3) shows a higher surface area (1,650 m^2/g) compared to AC without KOH impregnation (580 m^2/g). This may possibly be due to the addition of potassium into the carbon structure and intense gasification induced by extreme oxidation [55]. In conclusion, the development of a large surface area resulting from KOH activation can maximize the uptake of oil spills by the adsorbent. Shokry et al. [97] also studied the oil spill removal application using CS-based adsorbent. They reported coconut coil AC impregnated with KOH at the ratio of 1 : 2 (sample: KOH), carbonized at 600 °C, and activated at 800 °C exhibited surface area of only 691.8 m^2/g. By analyzing the results obtained by Raj and Joy and Shokry et al., a higher KOH activation ratio is more effective in developing an adsorbent with a larger surface area, thus enhancing the removal ability of the adsorbents.

Besides KOH, H_3PO_4 is also one of the most common activating agent uses for chemical activation purposes. Baharum et al. [94] used H_3PO_4 activation on CS-modified biochar to remove diazinon pesticides from an aqueous solution. The result showed that surface area and total pore volume achieved by CS-modified biochar with H_3PO_4 activation (surface area: 508.072 m^2/g, total pore volume: 0.203 cm^3/g) was higher than CS-modified biochar without chemical activation (surface area: 434.833 m^2/g, total pore volume: 0.174 cm^3/g). H_3PO_4 activation on CS-based adsorbent improved the porosity of structure, thus leading to better adsorption of adsorbent. Large pore volumes present in the adsorbent structure can perform rapid adsorption process. H_3PO_4 can be used as a cost-effective activating agent to enhance the surface area and increase the micropore volume of adsorbents so that adsorbent can attain the maximum adsorption capacity of pollutants.

Bhandari and Gogate [17] studied a similar concept on removing sodium dodecylbenzene by CS-based adsorbent. They reported that Thermo-chemical activation gave a larger surface area (674 m^2/g) compared to only chemically activated adsorbent (0.3667 m^2/g). Bhandari and Gogate explained that thermo-chemically activated adsorbent caused breaking of organic chains and a decrease in packing density [17]. The surface area increases when the pores open up to leave the carbon structure. Thermo-chemically activated CS-based adsorbent can attain large surface area and maximum sodium dodecylbenzene sulfonate adsorption capacity, which is beneficial for the pollutant removal process.

Physical activation also plays an important role in developing a better adsorbent for pollutants. Chandana et al. [90] conducted physical activation on CSAC to remove Cr(VI). The study showed that physical activation of CSAC with steam successfully achieved the largest surface area (610 m^2/g) compared to activation with carbon dioxide (523 m^2/g) and ozone (470 m^2/g). Chandana et al. [90] stated that partial oxidation of carbon by oxidizing gas such as steam and carbon dioxide increased the surface area, which favors the utilization of physical activation for the adsorption process. In summary, the literature study revealed that modification of CS-based adsorbents dramatically affects the surface morphology of adsorbents, especially changes in surface area and pore volume. Types of modifications also determine maximum adsorption capacity. Therefore, it is important to modify adsorbents with a suitable method to achieve a high adsorption capacity of pollutants.

ACTUAL WASTEWATER APPLICATION OF COCONUT SHELL BASED ADSORBENTS

The vast development of coconut industries has led to the disposal of CS waste into landfills and streams without appropriate treatment, which has become an environmental concern. Therefore, converting CS wastes into valuable adsorbents for industrial applications has become a great initiative. In the past years, many researchers have used CS in real wastewater treatment. Kaman et al. [98] conducted a batch adsorption study on POME using CSAC to reduce chemical oxygen demand (COD), total suspended solids (TSS), and color using CSAC. They carried out physical activation by using steam on CSAC and studied the effects of contact time and initial concentration on adsorption. The result showed that physically activated CSAC achieved a BET surface area of 744.118 m^2/g and pore volume of 0.4359 cm^3/g. Kaman et al. [98] also reported that CSAC gave the highest adsorption capacity for COD (10.215 mg/g), TSS (1.435 mg/g), and Color (63.291 PtCo/g). CSAC can meet the standard limit of Environmental Quality Act (EQA) ruled by the Department of Environment (DOE). Thus, CSAC is a promising candidate for POME treatment in palm oil

industries. In addition, Hayatu et al. [99] used CS-based adsorbent with microwave KOH activation at a ratio of 1.5 : 1 (KOH: char) to identify the feasibility of CS precursor for methane (CH_4) adsorption to overcome the challenge of compressed natural gas (CNG). They carried out the activation of CSAC using the microwave irradiation method at 500 W for 5 min and performed CH_4 adsorption at different pressures (4, 5, and 7 bar). The result showed that the amount of CH_4 uptake increased when pressure increased. In conclusion, CS wastes can be converted into adsorbents for CH_4 adsorption to replace CNG as fuel for vehicles, which adds value to the agricultural waste.

In addition, CS carbon was combined with limestone to explore the potential and effectiveness of modified CS carbon in removing the Cr(III) from wastewater solution, which was under the research area of Bakar et al. [100]. According to the World Health Organization (WHO), the concentration of Cr(III) in drinking water must meet the guideline where the value does not exceed 0.05 mg/L. Provisional guideline value of 0.05 mg/L is a safe drinking water standard that does not expose human health to a high risk of getting acute diseases [101]. Bakar et al. carried out an adsorption study to identify contact time and pH influences on the CS carbon/lime stone adsorption capacity. CS carbon/limestone achieved up to 98% of Cr(III) removal percentage at optimum pH of 5, agitation at 250 rpm, and 60 min of contact time by mixing CS carbon and limestone as adsorbent. In summary, mixing CS carbon and limestone has excellent potential to become an effective adsorbent to reduce Cr(III) concentration in industries.

Modification of CS into adsorbents also became the main concern for the leather tanning industry. Leather industrial wastewater contains harmful chemical materials, especially metallic chrome (Cr). Liquid waste quality was tested with (Cr: 0.5 mg/l, BOD: 128 mg/l, COD: 1,146.08 mg/l) and without (Cr: 644.85 mg/l, BOD: 1,200.1 mg/l, COD: 3,400 mg/l) treatment plant but failed to meet with quality standard determined by Regulation of DIY Governor number 7/2010 (Cr: 0.4 mg/l, BOD: 40 mg/l, COD: 90 mg/l). To deal with the pollution caused by the leather tanning industry, Lasindrang et al. [89] coated chitosan on CS active charcoal to increase adsorptive ability in removing Cr. Biological oxygen demand (BOD) and chemical oxygen demand (COD). Chitosan is an effective bio-adsorbent because it contains free amino groups and has high deacetylation rate capable of binding heavy metals. However, chitosan has lower adsorption ability at low pH due to protonation and is greatly affected by anions in the solution. In contrast, active charcoal has an amphoteric characteristic that depends on the pH of the solution to adsorb pollutants. Therefore, in this study, Lasindrang et al. [89] developed chitosan-coated CS active charcoal and studied the effects of pH and concentration of adsorbent on the measurement of Cr, BOD and COD. Lasindrang et al. [89] reported that chitosan-coated CS active charcoal successfully removed 99.19% of Cr, 99.95% of BOD, and 99.825% of COD. The results showed that chitosan-coated CS active charcoal is an effective adsorbent that can reduce >99% of chemical parameters obtained from leather industrial wastewater. The literature justified the potential of CS-based adsorbents for treating actual wastewater, including POME, CH_4, Cr(III) and metallic Cr adsorption. The broad utilization of CS wastes for industrial applications is mainly due to its feasibility as an adsorbent to replace the usage of high-cost commercial AC [89].

ENVIRONMENTAL AND ECONOMICAL PERSPECTIVE OF CONVERTING COCONUT SHELL INTO ADSORBENT

Carbonaceous CS is a high potential precursor to prepare adsorbents for wastewater treatment because it manages to reduce the release of greenhouse gases and also minimizes the severe issue of global warming. The main environmental concern is that when CS is disposed in the landfill, open burning of CS wastes produces large amount of CO_2 and CH_4, which has devastating impacts on both humans and the environment. Recently, the vast growth of the industrial field has caused critical environmental issues such as the emission of heat-trapping greenhouse gases such as CO_2, chlorofluorocarbon (CFC), CH_4, etc. [102]. Moreover, a concentrated amount of CO_2 gas in the atmosphere has caused a sudden increase in global temperature, leading to global warming, climate change, and ocean level rise [103]. Therefore, the adsorption method is an initiative to reduce the harmful effects caused by high CO_2 concentration by capturing the excess amount of CO_2. Furthermore, the adsorption process only requires low energy consumption, simple operation, and low cost, and is applicable over a wide range of experimental conditions such as temperature and pressure [45].

Carbonaceous CS is an ideal precursor to prepare AC for CO_2 gas adsorption because CS has high volatile content, low ash content, and high density, which meet raw material requirements to develop an effective adsorbent [42]. Huang et al. [102] stated that high porosity and large BET surface area of CS are also essential requirements in selecting it as raw material during adsorbent preparation. They compared the CO_2 adsorption capacity between CSAC and commercial AC under similar conditions ($T_{activation}$= 1,000 °C, $t_{activation}$=120 min). As a result, they found that the removal of CO_2 for CSAC was 14.3 mg/L while commercial AC was only 13.2 mg/L. Huang et al. explained that CSAC had a higher BET surface area (824 m^2/g) than commercial AC (800 m^2/g) at $T_{activation}$= 1,000 °C and $t_{activation}$=120 min [102]. The result indicates that a larger surface area contributes to higher adsorption capacity. However, the adsorption capability of both CSAC and commercially prepared AC dropped to 1.9 and 1.7 mg/L after 30 min. Huang et al. explained that CO_2 particles filled up most of the pores. This study concludes that CSAC possesses better characteristics and performance in adsorbing CO_2 gas than commercially prepared AC. Therefore, CS-based adsorbents can be applied to reduce severe environmental issues.

The industrial revolution caused tremendous energy demand, and fossil fuel is one source that provides energy worldwide. However, the combustion of fossil fuels has led to a rise in CO_2 concentration to around 413 ppm in 2020. Accumulation of excessive CO_2 has given rise to global warming issues. Therefore, the production of energy from organic waste such as CS and microbial fuel cells (MFCs) as an alternative energy supply solution is increasing demand [104]. MFCs can transform chemical energy into electrical energy [105]. For the working principle, cathode, the (oxygen) catalyst determines the efficiency and operation cost of MFCs.

Therefore, a highly effective oxygen catalyst is essential for the excellent performance of MFCs. Koo et al. [106] reported that AC is a promising oxygen catalyst due to its low cost ($1.4 kg^{-1}) compared to platinum, costing $625 g^{-1}. Reduction in the price of AC is possible by converting agricultural waste such as CS wastes into AC. The cost-effectiveness and simple operation method of adsorption in developing agricultural wastes-based adsorbents justify the utilization of CSAC as oxygen catalyst in MFCs systems [7]. However, the electro-catalytic activity of AC is low for the oxygen reduction reaction. Therefore, a metal-nitrogen-carbon (M-N-C) framework with high porosity was proposed to modify the AC and improve the catalytic performance. Koo et al. prepared the AC by combining it with the cobalt-nitrogen framework through ultrasonication and solution precipitation method [106]. The results revealed that when active sites for oxygen reduction reaction increased, charge transfer impedance decreased, and the reaction rate improved.

In addition, Koo et al. [107] reported that enhancement of cathodic performance can improve the electrical power generation by MFCs. Carbon black is the standard material used as conductive supporting material in AC-based cathode. However, Koo et al. discovered that replacing carbon black with reduced graphene oxide at the ratio of 1 : 1 could further improve cathodic performance due to having five times greater electrical conductivity and broader shape [107]. Furthermore, the introduction of current collectors could enhance the cathodic performance of MFCs, which are made from stainless steel, as reported by Nam et al. [108]. The study revealed that cathodic charge transfer impedance decreased up to 39%, which significantly helps to increase the effectiveness of oxygen reduction reaction. Besides cathodic performance, Jung et al. [109] stated that current metal collectors could also improve anodic performance. Their study introduced two types of current collectors: titanium wires and stainless steel mesh. The result showed that carbon-felt anode with stainless steel mesh is advantageous in short-term performance due to having a more prominent collector, but not for long-term performance due to interference with mass transfer and microbial growth. On the other hand, a carbon-felt anode with titanium wires is advantageous in long-term performance. Therefore, the introduction of stainless steel could further enhance the cathodic performance but not the anodic performance. Besides energy production, MFCs are implemented for wastewater treatment in the next generation. They reported that anode arrangement plays a significant role [110,111] in maximizing the capability of MFCs to treat wastewater and produce energy. The result revealed that agricultural CS waste-based AC as an oxygen catalyst is advantageous from economical and environmental perspectives.

Moreover, Arena et al. [112] considered the environmental perspective in their study. They assessed the input and output during the production of CSAC through the life cycle assessment (LCA). The inputs included resources and energy, while output included the emission of waste products to the environment. Arena et al. [112] demonstrated different scenarios to observe the environmental performance of AC. Different scenarios were referring to scenario 1 (utilization of coconut shell for electric energy production in Indonesia), scenario 2 (release of distillate product from carbonization process to the atmosphere), scenario 3 (allocation of AC production in-country nearby to Indonesia), and scenario 4 (utilization of CS for both activated carbon and electric energy production). As a result, the analysis showed that the reduction of global warming potential reached around 80%. Furthermore, cost reduction is possible when the CS wastes are used as biofuel generators for other needs, referring to scenario 4 conducted by [112]. This study concluded that AC developed from biomass such as CS is beneficial in reducing environmental issues such as global warming by reducing the use of electrical energy during the process and by utilizing the electrical energy produced by biomass material.

The cost of adsorbents is a significant criteria when choosing an effective adsorbent because it has a considerable impact on a modal for operating the adsorption process. Commercial AC is widely used in adsorption, but a high cost is required for manufacturing due to increased electricity usage during production [113]. According to Sigma Aldrich (2019), the cost of commercially prepared activated carbon is RM 596.00/kg. This expense can be a financial issue for industrial applications because large quantities of adsorbents are needed. So, various studies of converting CS waste into useful adsorbents aim to replace the use of commercial AC. The economic perspective survey has been investigated by comparing different adsorbents in removing Cr(IV) ions. Babel and Kurniawan [114] reported that the commercial price of CSAC per kg is US$0.34, while the price for commercial AC is US$1.37 and chitosan is US$1.14. The result showed that 1 kg of CSAC treated with nitric acid successfully removed 10.88 g of Cr (IV) ions, which only cost US$0.34. In comparison, 1 kg of commercial AC successfully removed 15.47 g of Cr(IV) ions, but it required US$ 1.37 to remove such an amount of Cr(IV) ions from an aqueous solution. Without considering the costs involved in operation, transportation, maintenance of adsorbents, CSAC is more beneficial than commercially prepared AC in removing Cr(IV) ions. In summary, the development of CS wastes-based adsorbents is beneficial from an environmental and economic perspective, meeting the need for large-scale industrial applications.

CONCLUSION

This review gives an overall view of the feasibility of carbonaceous CS as a precursor material to develop adsorbents for wastewater treatment applications. Preparation of CS-based adsorbents has two fundamental steps: carbonization and activation. Both carbonization and activation processes have significant impact on the adsorbent's structure. As discussed in this review, different synthesis methods of CS-based adsorbents from the previous studies have given other researchers significant insight to choose the suitable modification method for developing an effective adsorbent. Till date, studies on hybrid CS-based adsorbents are still lacking. Therefore, research in finding the effective metallic materials to hybrid with CS-based adsorbents should be the main focus because the selection of precursors significantly impacts the adsorption performance of the adsorbents. This review also discussed the perspectives from environmental and economic viewpoints in utilizing CS-based adsorbents. Development of green adsorbents from agricultural wastes is an exciting technique used for wastewater treat-

ment to replace the utilization of commercially prepared and high-cost AC in the adsorption process to keep the principle of green chemistry. Besides recalcitrant pollutants in aqueous solution, CS-based adsorbents are ideal in reducing the concentration of carbon dioxide gas, which has caused a severe global issue. From comprehensive studies, CS-based adsorbents are high potential candidates for large-scale usage in industries to treat contaminated wastewater due to their unique properties, such as being environmentally friendly, cost-effective and abundantly available. The environmental and economic perspectives of converting CS into adsorbents are also the main concerns in preparing adsorbents to avoid secondary pollution and high operation cost.

ACKNOWLEDGEMENT

The authors are grateful to Ministry of Higher Education for providing financial support via Fundamental Research Grant Scheme (FRGS/1/2019/TK05/UM/01/3).

DECLARATION OF COMPETING INTEREST

The authors declare that they have no known competing financial interests or personal relationships that could have appeared to influence the work reported in this paper.

CONFLICT OF INTEREST

The authors declare that there are no conflicts of interest in this work.

ABBREVIATIONS

-OH : hydroxyl
AC : activated carbon
AgNPs : Silver Nanoparticles
BB 3 : Basic Blue 3
BET : Brunauer-Emmett-Teller
BG : Brilliant Green
BOD : Biological Oxygen Demand
BR 14 : Basic Red 14
BY 13 : Basic Yellow 13
C-H : carbon hydrogen bond
C=C : carbon carbon double bond
C=O : carbonyl
CAC/$CoFe_2O_4$: coconut activated carbon/cobalt ferrite
CC : carbon content
CFC : chlorofluorocarbon
CH_4 : methane
CNG : compressed natural gas
Co : Fe : CAC : cobalt : iron : coconut activated carbon
CO_2 : carbon dioxide
COD : chemical oxygen demand
Cr : chrome
CR : congo red
CS : coconut shell
CSAC : coconut shell activated carbon
CSF/Mg-Al : coconut shell fibre/magnesium-aluminium
CuO-NPs : copper oxide nanoparticles
CV : crystal violet
DOE : department of environment
DY 12 : Direct Yellow 12
DY 12B : Direct Yellow 12B
EB : eriochrome black
EQA : environmental quality act
FTIR : fourier transform infrared spectroscopy
H-H : hydrogen bond
H_2O : water
H_2SO_4 : sulfuric acid
H_3PO_4 : phosphoric acid
HCl : hydrochloric acid
HTC : hydrothermal carbonization
LCA : life cycle assessment
MB : methylene blue
MFCs : microbial fuel cells
MG : malachite green
MO : methyl orange
MS : municipal sludge
NaOH : sodium hydroxide
Pb^{2+} : Lead (II) ion
POME : palm oil mill effluent
RB 19 : Reactive Blue 19
RBBR : remazol brilliant blue R
SA : surface area
SEM/EDS : scanning electron microscopy/energy dispersive spectroscopy
SS : sewage sludge
SSAC : sewage sludge activated carbon
TSS : total suspended solids
VC : volatile content
WHO : World Health Organization
$ZnCl_2$: zinc chloride

REFERENCES

1. T. Askun, N. Ya'acob, M. Abdullah, M. Ismail, M. Medina, T. L. Talarico, I. A. Casas, T. C. Chung, W. J. Dobrogosz, L. Axelsson, S. E. Lindgren, W. J. Dobrogosz, L. Kerkeni, P. Ruano, L. L. Delgado, S. Picco, L. Villegas, F. Tonelli, M. Merlo, J. Rigau, D. Diaz and M. Masuelli, *InTech.*, **32**, 137 (2018).
2. M. U. Mahidin, Selected Agric. Indicators, 2019 (2021).
3. A. Neh and N. E. H. Ali, *Open Access J. Waste Manag. Xenobiotics.*, **3**, 1 (2020).
4. X. J. Tan, W. L. Cheor, K. S. Yeo and W. Z. Leow, *J. King Saud Univ. - Comput. Inf. Sci.*, **34**, 1569 (2022).
5. H. A. Umar, S. A. Sulaiman, M. A. Meor Said, A. Gungor, M. Shahbaz, M. Inayat and R. K. Ahmad, *Biomass Bioenergy*, **151**, 106179 (2021).
6. N. Tripathi, C. D. Hills, R. S. Singh and C. J. Atkinson, *Npj Clim. Atmos. Sci.*, **2**, 1 (2019).
7. A. Azari, R. Nabizadeh, A. H. Mahvi and S. Nasseri, *Int. J. Environ. Anal. Chem.*, 1 (2020).
8. Y. Rashtbari, S. Hazrati, A. Azari, S. Afshin, M. Fazlzadeh and M.

Vosoughi, *Adv. Powder Technol.*, **31**, 1612 (2020).
9. M. Heydari Moghaddam, R. Nabizadeh, M. H. Dehghani, B. Akbarpour, A. Azari and M. Yousefi, *Microchem. J.*, **150**, 104185 (2019).
10. A. Azari, M. Yeganeh, M. Gholami and M. Salari, *J. Hazard. Mater.*, **418**, 126348 (2021).
11. A. Azari, A. A. Babaei, R. Rezaei-Kalantary, A. Esrafili, M. Moazzen and B. Kakavandi, *J. Maz. Univ. Med. Sci.*, **23**, 14 (2014).
12. E. Ahmadi, B. Kakavandi, A. Azari, H. Izanloo, H. Gharibi, A. H. Mahvi, A. Javid and S. Y. Hashemi, *Desalin. Water Treat.*, **57**, 27768 (2016).
13. M. A. Ahmad, M. A. Eusoff, P. O. Oladoye, K. A. Adegoke and O. S. Bello, *Chem. Data Collect.*, **32**, 1 (2021).
14. G. Vyavahare, P. Jadhav, J. Jadhav, R. Patil, C. Aware, D. Patil, A. Gophane, Y. H. Yang and R. Gurav, *J. Clean. Prod.*, **207**, 296 (2019).
15. O. Oribayo, O. O. Olaleye, A. S. Akinyanju, K. O. Omoloja and S. O. Williams, *Niger. J. Technol.*, **39**, 1076 (2021).
16. L. P. Hoang, H. T. Van, T. T. Hang Nguyen, V. Q. Nguyen and P. Q. Thang, *J. Chem.*, **2020**, 1 (2020).
17. P. S. Bhandari and P. R. Gogate, *Desalin. Water Treat.*, **165**, 111 (2019).
18. C. Song, S. Wu, M. Cheng, P. Tao, M. Shao and G. Gao, *Sustainability*, **6**, 86 (2014).
19. M. Abdulsalam, C. M. Hasfalina, H. A. Mohamed, S. F. Abd Karim and M. S. Faiez, *Food Res.*, **2**, 526 (2018).
20. Y. Dai, Q. Sun, W. Wang, L. Lu, M. Liu, J. Li, S. Yang, Y. Sun, K. Zhang, J. Xu, W. Zheng, Z. Hu, Y. Yang, Y. Gao, Y. Chen, X. Zhang, F. Gao and Y. Zhang, *Chemosphere*, **211**, 235 (2018).
21. M. A. Islam, M. J. Ahmed, W. A. Khanday, M. Asif and B. H. Hameed, *J. Environ. Manage.*, **203**, 237 (2017).
22. M. A. Yahya, Z. Al-Qodah and C. W. Z. Ngah, *Renew. Sustain. Energy Rev.*, **46**, 218 (2015).
23. R. Bushra, S. Mohamad, Y. Alias, Y. Jin and M. Ahmad, *Micropor. Mesopor. Mater.*, **319**, 111040 (2021).
24. I. Guerrero-Coronilla, L. Morales-Barrera and E. Cristiani-Urbina, *J. Environ. Manage.*, **152**, 99 (2015).
25. C. A. Riyanto and E. Prabalaras, *J. Phys. Conf. Ser.*, **1307**, 012002 (2019).
26. A. A. Moosa, A. M. Ridha and N. A. Hussien, *Am. J. Mater. Sci.*, **6**, 115 (2016).
27. Y. Omidi Khaniabadi, H. Basiri, A. Jafari, S. Saeedi, G. Goudarzi, F. Taheri and M. Salehi Murkani, *Jundishapur J. Heal. Sci.*, **10**, 1 (2016).
28. M. A. Ahmad, N. B. Ahmed, K. A. Adegoke and O. S. Bello, *Chem. Data Collect.*, **31**, 100578 (2021).
29. T. H. Do, V. T. Nguyen, N. Q. Dung, M. N. Chu, D. Van Kiet, T. T. K. Ngan and L. Van Tan, *Mater. Today Proc.*, **38**, 3405 (2020).
30. F. Bin Abdurrahman, M. Akter and M. Z. Abedin, *Int. J. Sci. Technol. Res.*, **2**, 47 (2013).
31. M. E. Fernandez, G. V. Nunell, P. R. Bonelli and A. L. Cukierman, *Ind. Crops Prod.*, **62**, 437 (2014).
32. S. Dey, S. R. Basha, G. V. Babu and T. Nagendra, *Clean. Mater.*, **1**, 100001 (2021).
33. W. Saadi, S. Rodríguez-Sánchez, B. Ruiz, S. Najar-Souissi, A. Ouederni and E. Fuente, *J. Environ. Chem. Eng.*, **10**, 107010 (2022).
34. M. K. Dahri, M. R. R. Kooh and L. B. L. Lim, *J. Environ. Chem. Eng.*, **2**, 1434 (2014).
35. M. K. Uddin and A. Nasar, *Sci. Rep.*, **10**, 1 (2020).
36. A. M. Aljeboree, A. N. Alshirifi and A. F. Alkaim, *Arab. J. Chem.*, **10**, S3381 (2017).
37. T. K. Hoe, *Plant. Kuala Lumpur*, **94**, 413 (2018).
38. I. Emahi, P. O. Sakyi, P. Bruce-Vanderpuije and A. R. Issifu, *Environ. Nat. Resour. Res.*, **9**, 127 (2019).
39. T. D. Gunawan, Mariana, E. Munawar and S. Muchtar, *Mater. Today Proc.*, **63**, S40 (2022).
40. E. H. Sujiono, D. Zabrian, Zurnansyah, Mulyati, V. Zharvan, Samnur and N. A. Humairah, *Results Chem.*, **4**, 100291 (2022).
41. R. Kabir Ahmad, S. Anwar Sulaiman, S. Yusup, S. Sham Dol, M. Inayat and H. Aminu Umar, *Ain Shams Eng. J.*, **13**, 101499 (2022).
42. S. N. Dongardive, A. G. Mohod and Y. P. Khandetod, *Int. J. Eng. Innov. Technol.*, **12**, 94 (2019).
43. R. Maniarasu, S. K. Rathore and S. Murugan, *IOP Conf. Ser. Mater. Sci. Eng.*, **1130**, 012022 (2021).
44. H. U. Itodo and A. U. Itodo, *J. Chem. Pharm. Resour.*, **2**, 673 (2010).
45. D. Das, D. P. Samal, M. BC, *J. Chem. Eng. Process Technol.*, **6**, 1000248 (2015).
46. F. Ronsse, R. W. Nachenius and W. Prins, *Recent Adv. in Thermochem. Convers. of Biomass*, 293 (2015).
47. R. K. Liew, E. Azwar, P. N. Y. Yek, X. Y. Lim, C. K. Cheng, J. H. Ng, A. Jusoh, W. H. Lam, M. D. Ibrahim, N. L. Ma and S. S. Lam, *Bioresour. Technol.*, **266**, 1 (2018).
48. B. Yang, Y. Liu, Q. Liang, M. Chen, L. Ma, L. Li, Q. Liu, W. Tu, D. Lan and Y. Chen, *Ecotoxicol. Environ. Saf.*, **170**, 722 (2019).
49. C. Ooi, T. Lee, S. Pung and F. Yeoh, *ASEAN Eng. J.*, **4**, 40 (2013).
50. K. Yang, J. Peng, H. Xia, L. Zhang, C. Srinivasakannan and S. Guo, *J. Taiwan Inst. Chem. Eng.*, **41**, 367 (2010).
51. K. U. Devens, S. P. Neto, D. L. D. A. Oliveira and M. S. Gonçalves, *Rev. Virtual Quim.*, **10**, 288 (2018).
52. M. H. Samsudin, M. A. Hassan, J. Idris, N. Ramli, M. Z. Mohd Yusoff, I. Ibrahim, M. R. Othman, A. A. Mohd Ali and Y. Shirai, *Waste Manag. Res.*, **37**, 551 (2019).
53. W. T. Tsai and T. J. Jiang, *Biomass Convers. Biorefinery*, **8**, 711 (2018).
54. M. Jin, B. Hu, X. Tang, L. Zou and G. Yu, *IOP Conf. Ser. Earth Environ. Sci.*, **446**, 3 (2020).
55. K. G. Raj and P. A. Joy, *J. Environ. Chem. Eng.*, **3**, 2068 (2015).
56. W. Li, K. Yang, J. Peng, L. Zhang, S. Guo and H. Xia, *Ind. Crops Prod.*, **28**, 190 (2008).
57. A. A. Azzaz, B. Khiari, S. Jellali, C. M. Ghimbeu and M. Jeguirim, *Renew. Sustain. Energy Rev.*, **127**, 109882 (2020).
58. W. Tu, Y. Liu, Z. Xie, M. Chen, L. Ma, G. Du and M. Zhu, *J. Colloid Interface Sci.*, **593**, 390 (2021).
59. E. Danso-Boateng, A. S. Mohammed, G. Sander, A. D. Wheatley, E. Nyktari and I. C. Usen, *SN Appl. Sci.*, **3**, 1 (2021).
60. M. Kiliç, E. Apaydin-Varol and A. E. Pütün, *Appl. Surf. Sci.*, **261**, 247 (2012).
61. T. L. Silva, A. Ronix, O. Pezoti, L. S. Souza, P. K. T. Leandro, K. C. Bedin, K. K. Beltrame, A. L. Cazetta and V. C. Almeida, *Chem. Eng. J.*, **303**, 467 (2016).
62. U. D. Hamza, N. S. Nasri, N. A. S. Amin, J. Mohammed and H. M. Zain, *Desalin. Water Treat.*, **57**, 7999 (2016).
63. K. Sun and J. chun Jiang, *Biomass Bioenergy*, **34**, 539 (2010).
64. C. Patra, R. Gupta, D. Bedadeep and S. Narayanasamy, *Environ. Pollut.*, **266**, 115102 (2020).
65. A. H. Jawad, A. S. Abdulhameed and M. S. Mastuli, *J. Taibah Univ. Sci.*, **14**, 305 (2020).

66. A. H. Jawad, A. Saud Abdulhameed, L. D. Wilson, S. S. A. Syed-Hassan, Z. A. ALOthman and M. Rizwan Khan, *Chinese J. Chem. Eng.*, **32**, 281 (2021).
67. R. S. Piriya, R. M. Jayabalakrishnan, M. Maheswari, K. Boomiraj and S. Oumabady, *Water Sci. Technol.*, **83**, 1167 (2021).
68. H. K. Yağmur and İ. Kaya, *J. Mol. Struct.*, **1232**, 130071 (2021).
69. M. Lutfi, Hanafi, B. Susilo, J. Prasetyo, Sandra and U. Prajogo, *IOP Conf. Ser. Earth Environ. Sci.*, **733**, 012134 (2021).
70. X. Wang, D. Li, W. Li, J. Peng, H. Xia, L. Zhang, S. Guo and G. Chen, *BioResources*, **8**, 6184 (2013).
71. A. Rehman, M. Park and S. J. Park, *Coatings*, **9**, 1 (2019).
72. I. A. W. Tan, M. O. Abdullah, L. L. P. Lim and T. H. C. Yeo, *J. Appl. Sci. Process Eng.*, **4**, 186 (2017).
73. A. L. Cazetta, A. M. M. Vargas, E. M. Nogami, M. H. Kunita, M. R. Guilherme, A. C. Martins, T. L. Silva, J. C. G. Moraes and V. C. Almeida, *Chem. Eng. J.*, **174**, 117 (2011).
74. J. Mohammed, N. S. Nasri, M. A. A. Zaini, U. D. Hamza, H. M. Zain and F. N. Ani, *Desalin. Water Treat.*, **57**, 7881 (2016).
75. X. Wang, X. Zhou, W. Chen, M. Chen and C. Liu, *R. Soc. Open Sci.*, **6**, 180872 (2019).
76. K. Sun, C. Y. Leng, J. C. Jiang, Q. Bu, G. F. Lin, X. C. Lu and G. Z. Zhu, *Xinxing Tan Cailiao/New Carbon Mater.*, **32**, 451 (2017).
77. H. T. Van, T. M. P. Nguyen, V. T. Thao, X. H. Vu, T. V. Nguyen and L. H. Nguyen, *Water. Air. Soil Pollut.*, **229**, 1 (2018).
78. A. K. Prajapati and M. K. Mondal, *J. Mol. Liq.*, **307**, 112949 (2020).
79. S. Amelia, W. B. Sediawan, Z. Mufrodi and T. Ariyanto, *J. Bahan Alam Terbarukan*, **7**, 164 (2019).
80. L. Ai, H. Huang, Z. Chen, X. Wei and J. Jiang, *Chem. Eng. J.*, **156**, 243 (2010).
81. Y. D. Liang, Y. J. He, T. T. Wang and L. H. Lei, *J. Water Process Eng.*, **27**, 77 (2019).
82. S. Moosavi, R. Y. M. Li, C. W. Lai, Y. Yusof, S. Gan, O. Akbarzadeh, Z. Z. Chowhury, X. G. Yue and M. R. Johan, *Nanomaterials*, **10**, 1 (2020).
83. L. Li, S. Liu and J. Liu, *J. Hazard. Mater.*, **192**, 683 (2011).
84. J. Romanos, M. Beckner, T. Rash, L. Firlej, B. Kuchta, P. Yu, G. Suppes, C. Wexler and P. Pfeifer, *Nanotechnology*, **23**, 015401 (2012).
85. R. H. Khuluk, A. Rahmat, Buhani and Suharso, *Indones. J. Sci. Technol.*, **4**, 229 (2019).
86. U. A. Isah, G. Abdulraheem, S. Bala, S. Muhammad and M. Abdullahi, *Int. Biodeterior. Biodegrad.*, **102**, 265 (2015).
87. S. Srisorrachatr, P. Kri-Arb, S. Sukyang and C. Jumruen, *MATEC Web Conf.*, **119**, 01019 (2017).
88. E. Altıntıg, M. Yenigun, A. Sarı, H. Altundag, M. Tuzen and T. A. Saleh, *Environ. Technol. Innov.*, **21**, 101305 (2021).
89. M. Lasindrang, H. Suwarno, S. D. Tandjung and H. N. Kamiso, *Agric. Agric. Sci. Procedia*, **3**, 241 (2015).
90. L. Chandana, K. Krushnamurty, D. Suryakala and C. Subrahmanyam, *Mater. Today Proc.*, **26**, 44 (2018).
91. A. Jayan, *Int. Res. J. Eng. Technol.*, **6**, 3464 (2019).
92. J. Yuan, Y. Zhu, J. Wang, L. Gan, M. He, T. Zhang, P. Li and F. Qiu, *Food Bioprod. Process.*, **126**, 293 (2021).
93. U. Anwana Abel, G. Rhoda Habor and O. Innocent Oseribho, *Am. J. Chem. Eng.*, **8**, 36 (2020).
94. N. A. Baharum, H. M. Nasir, M. Y. Ishak, N. M. Isa, M. A. Hassan and A. Z. Aris, *Arab. J. Chem.*, **13**, 6106 (2020).
95. J. Kodali, S. Talasila, B. Arunraj and R. Nagarathnam, *Case Stud. Chem. Environ. Eng.*, **3**, 100099 (2021).
96. A. Q. Alorabi, M. Shamshi Hassan and M. Azizi, *Arab. J. Chem.*, **13**, 8080 (2020).
97. H. Shokry, M. Elkady and H. Hamad, *J. Mater. Res. Technol.*, **8**, 4477 (2019).
98. S. P. D. Kaman, I. A. W. Tan and L. L. P. Lim, *MATEC Web Conf.*, **87**, 1 (2016).
99. U. S. Hayatu, N. S. Nasri, H. M. Zain, A. A. Bdulrahman and N. M. Rashid, *Chem. Eng. Trans.*, **61**, 1249 (2017).
100. A. A. A. Bakar, N. F. A. Razak, N. A. Akbar, N. M. Daud and K. A. M. Ali, *IOP Conf. Ser. Earth Environ. Sci.*, **646**, 012063 (2021).
101. WHO, Who., WHO/SDE/WS, WHO/SDE/WSH/05.08/10, http://www.who.int/water_sanitation_health/dwq/chemicals/mercuryfinal.pdf (2005).
102. P. H. Huang, H. H. Cheng and S. H. Lin, *J. Chem.*, **2015**, 1 (2015).
103. K. A. Ali, M. I. Ahmad and Y. Yusup, *Sustainability*, **12**, 7427 (2020).
104. P. Dange, N. Savla, S. Pandit, R. Bobba, S. P. Jung, P. K. Gupta, M. Sahni and R. Prasad, *J. Renew. Mater.*, **10**, 665 (2022).
105. H. V. H. Tran, E. Kim and S. P. Jung, *J. Ind. Eng. Chem.*, **106**, 269 (2022).
106. B. Koo and S. P. Jung, *Chem. Eng. J.*, **424**, 130388 (2021).
107. B. Koo, S. M. Lee, S. E. Oh, E. J. Kim, Y. Hwang, D. Seo, J. Y. Kim, Y. H. Kahng, Y. W. Lee, S. Y. Chung, S. J. Kim, J. H. Park and S. P. Jung, *Electrochim. Acta*, **297**, 613 (2019).
108. T. Nam, S. Son, E. Kim, H. V. H. Tran, B. Koo, H. Chai, J. Kim, S. Pandit, A. Gurung, S. E. Oh, E. J. Kim, Y. Choi and S. P. Jung, *Environ. Eng. Res.*, **23**, 383 (2018).
109. S. P. Jung, E. Kim and B. Koo, *Chemosphere*, **209**, 542 (2018).
110. T. Nam, H. Kang, S. Pandit, S. H. Kim, S. Yoon, S. Bae and S. P. Jung, *J. Clean. Prod.*, **277**, 124125 (2020).
111. H. Kang, J. Jeong, P. L. Gupta and S. P. Jung, *Int. J. Hydrogen Energy*, **42**, 27693 (2017).
112. N. Arena, J. Lee and R. Clift, *J. Clean. Prod.*, **125**, 68 (2016).
113. A. R. A. Rahim, Iswarya, K. Johari, N. Shehzad, N. Saman and H. Mat, *Environ. Eng. Res.*, **26**, 200250 (2020).
114. S. Babel and T. A. Kurniawan, *Chemosphere*, **54**, 951 (2004).